

ACCURACY ASSESSMENT OF TERRESTRIAL LASER SCANNING AND
DIGITAL CLOSE RANGE PHOTOGRAMMETRY FOR 3D CULTURAL HERITAGE

by

Abdullah Taha Ahmed Albourae

Bachelor of Architecture
Faculty of Environmental Designs at King Abdul Aziz University
Jeddah, Kingdom of Saudi Arabia, 2008

A thesis

presented to Ryerson University

in partial fulfillment of the requirements for the degree of
Master of Applied Science

in the program of
Civil Engineering (Geomatics Engineering)

Toronto, Ontario, Canada, 2014
©Abdullah Taha Ahmed Albourae 2014

Author's Declaration

I hereby declare that I am the sole author of this thesis. This is a true copy of the thesis, including any required final revisions, as accepted by my examiners.

I authorize Ryerson University to lend this thesis to other institutions or individuals for the purpose of scholarly research.

I further authorize Ryerson University to reproduce this thesis by photocopying or by other means, in total or in part, at the request of other institutions or individuals for the purpose of scholarly research.

I understand that my thesis may be made electronically available to the public.

Abstract

There are various surveying techniques used in the field of cultural heritage documentation. Close Range Photogrammetry (CRP) and Terrestrial Laser Scanning (TLS) techniques have been widely used in 3D modeling applications. Various research studies integrate these techniques to enhance the quality of the data acquired. The main objective of this research is to assess the accuracy of TLS and CRP. The two methods are applied to two culture heritage case studies, which are located in the historic district in Jeddah, Saudi Arabia. The data obtained from both techniques is compared with data captured using traditional surveying techniques as reference data. The results show that TLS tends to be more accurate than CRP. In the first case study (Bab Makkah), CRP and TLS produced 0.044 m and 0.008 m overall RMS error, respectively; while CRP produced 0.025 m and TLS produced 0.021 m in the second case study (Bab Sharif).

Acknowledgements

First, I am very grateful to the almighty Allah, the gracious and the merciful, for this accomplishment. A special thank to my Dad and Mom as they are always my inspiration and solid source of support. Also, to all of my sisters and brothers, many thanks for your care and support. Finally, and most importantly, many thanks to my dear wife for her patience and support throughout my studies.

A special thanks to all staff members of the Geomatics Department in the Faculty of Environmental Designs at King Abdul Aziz University, who supported me by providing all instruments needed for this study. In addition, I'd like to thank the Saudi Arabian Cultural Bureau in Canada, who facilitated my Canadian study term. I dedicate this work to my country, The Kingdom of Saudi Arabia, and I sincerely hope that this thesis helps to improve the heritage preservation methods in my country.

I should also thank my supervisor, Dr. Ahmed Shaker, for his unabated advice and careful guidance despite his extremely busy schedule. I'd like to further thank my thesis committee: Prof. Songnian Li, Dr. Darko Joksimovic, and Dr. Serhan Guner, for their suggestions and insightful comments. My sincere thanks also goes to the Graduate Program Director, Dr. Ahmed El-Rabbany, for his care and advice during my Master's degree.

Finally, I would like to express my gratitude to Dr. Wai Yeung Yan for his continuous support to help me finalize my thesis; and also, to all of my friends and colleagues in the Department of Civil Engineering for their help, consideration, and thoughts.

Table of Contents

Author's Declaration	ii
Abstract.....	iii
Acknowledgements.....	iv
List of Tables	vi
List of Figures.....	vii
CHAPTER 1: INTRODUCTION.....	1
1.1. Introduction.....	1
1.2. Problem Definition.....	1
1.3. Objectives	3
1.4. Thesis Structure	3
CHAPTER 2: BACKGROUND.....	4
2.1. Introduction.....	4
2.2. Close Range Photogrammetry (CRP)	4
2.3. Terrestrial Laser Scanning (TLS)	7
2.4. Traditional Survey Using Leica Smart-Station (LSS)	10
2.5. Close Range Photogrammetry (CRP) vs. Terrestrial Laser Scanning (TLS).....	11
2.6. Existing Studies of Heritage Documentation.....	12
2.6.1. The Use of CRP for Heritage Documentation.....	12
2.6.2. The Use of TLS for Heritage Documentation	13
2.6.3. CRP vs. TLS for Heritage Documentation.....	14
CHAPTER 3: METHODOLOGY	16
3.1. Introduction.....	16
3.2. Study Areas.....	16
3.3. General Workflow	18
3.4. Close Range Photogrammetry (CRP)	19
3.4.1. Data Acquisition for Bab Makkah and Bab Sharif.....	20
3.4.2. Data Processing of Image Calibration.....	21
3.4.2.1. Lab Camera Calibration.....	21
3.4.2.2. Field Camera Calibration.....	23
3.4.3. CRP Image Registration.....	24
3.5. Terrestrial Laser Scanning (TLS)	25
3.5.1. Data Acquisition.....	25
3.5.2. Data Processing	26
3.6. Traditional Surveying	29
CHAPTER 4: RESULTS AND ANALYSIS.....	30
4.1. CRP Results of Bab Makkah Dataset	30
4.2. CRP Results of Bab Sharif Dataset.....	31
4.3. TLS Results for Bab Makkah and Bab Sharif.....	32
4.4. Accuracy Assessment of Bab Makkah Results.....	33
4.5. Accuracy Assessment of Bab Sharif Results	38
CHAPTER 5: CONCLUSIONS	42
References.....	44

List of Tables

Table 2.1. Characteristics of photogrammetry and laser scanner data	11
Table 3.1. Camera specification	20
Table 4.1. Camera calibration results for Bab Makkah and Bab Sharif	32
Table 4.2. Comparison between LSS and CRP coordinates of the same targets.....	34
Table 4.3. Comparison between LSS and TLS coordinates of the same targets	36
Table 4.4. A summary of the accuracy assessment between CRP and TLS	37
Table 4.5. Accuracy assessment for Bab Sharif results.....	39
Table 4.6. A comparison of accuracy assessment achieved between CRP and TLS	41

List of Figures

Figure 2.1. Photogrammetry principle.....	4
Figure 2.2. An example of configuration for a bundle solution	5
Figure 2.3. The Collinearity condition	5
Figure 2.4. Concept of TLS measurments.....	7
Figure 2.5. The principle of the Tacheometric laser.....	8
Figure 2.6. The seven transformation parameters	9
Figure 2.7. An illustration of a traditional survey using LSS.....	10
Figure 3.1. The historical region of Jeddah (Bab Makkah & Sharif Gate).....	16
Figure 3.2. A pictogram illustration of general workflow.....	18
Figure 3.3. Research workflow	19
Figure 3.4. An illustration of close range photogrammetry concept.....	20
Figure 3.5. Multi-sheet lab camera calibration.....	22
Figure 3.6. The automatic calibration process in PhotoModeler.....	22
Figure 3.7. Example images used for field calibration.....	24
Figure 3.8. An illustration of the laser scanning configuration and the targets used.....	25
Figure 3.9. An illustration of the TLS in the Bab Sharif	26
Figure 3.10. The results of data registration for Bab Makkah.....	27
Figure 3.11. The results of data registration for Bab Sharif	28
Figure 3.12. An illustration of traditional survey methods using Leica Smart Station	29
Figure 4.1. The distribution of 20 artificial black and white targets on Bab Makkah.....	30
Figure 4.2. Four artificial targets that were assigned for image registration.....	31
Figure 4.3. CRP image processing for Bab Sharif	31
Figure 4.4. 3D model generation of Bab Makkah	33
Figure 4.5. 3D model generation of Bab Sharif	33
Figure 4.6. The RMS error produced by the CRP technique.....	35
Figure 4.7. The RMS error produced by the TLS technique.....	37
Figure 4.8. A comparison of RMS error between CRP and TLS.....	38

CHAPTER 1: INTRODUCTION

1.1.Introduction

Cultural heritage buildings play an important role in reflecting a country's identity. Recently, governments have directed their attention towards protecting cultural heritage buildings from war, natural disasters, and general wear and tear. In addition to individual countries, international organizations, such as the United Nations Organization of Education, Science and Culture (UNESCO), and its World Heritage Centre, are interested in documenting and preserving historical sites. Based on this increase demand, engineers have been seeking more efficient and cost effective methods to document these cultural heritage sites.

Rehabilitation and restoration of heritage buildings depends on being able to accurately record their measurements and details. In the last decade, the field of historic building documentation has developed competition between different surveying techniques, systems, and devices for accuracy, cost effectiveness, and overall efficiency. Two of the main documentation techniques are: Digital Close-Range Photogrammetry (CRP) and Terrestrial Laser Scanner (TLS).

1.2.Problem Definition

Heritage documentation is one of the official ways to give definition and recognition to cultural and historical infrastructure. Heritage documentation is used as an aid for protection, restoration, conservation, preservation, identification, monitoring, interpretation, and finally, management of historical buildings, sites, and cultural landscapes (Haddad and Akasheh, 2005). In the past, the heritage documentation mainly

relied on human interpretation and record keeping, such as hand drawings, on-site measurement, and sculptures. Documentation tools have undergone a major improvement over the past 20 years. However, these tools provide an additional way to capture the materials, colors, decorations, and so forth, in order to obtain more accurate results.

Digital photogrammetry and laser scanning are the two measurement techniques growing in the field of heritage documentation. Digital photogrammetry offers a rapid accurate method for acquiring three dimensional data, particularly related to large complex objects. Data processing software, such as PhotoModeler, can be used to extract accurate measurements and three dimension models from photographs (Haddad and Akasheh, 2005). Furthermore, laser scanners are used intensively for the generation of 3D models in a number of diverse areas, including: glacier monitoring, robotics navigation, and space exploration. Initially, it appears that laser technology has surpassed traditional close-range photogrammetry in accuracy and automation level.

In this study, two historic sites (Bab Makkah and Bab Sharif) in Saudi Arabia are surveyed and documented using digital photogrammetry and terrestrial laser scanning techniques. Due to their historical significance, availability of equipment and the uniqueness of structure, both gates remain in their original position, which is now situated in the middle of street intersections. Built in the 15th century, these gates still attract a lot of attention from tourists and authorities; and thus, their appearance and maintenance are very important. Furthermore, these gates serve a purpose in the Islamic tradition, in that they have outstanding geometrical details, which reflect the city's identity.

1.3.Objectives

Natural disasters, erosion, war, neglect, and conflicts of interest result in an urgent need to document heritage sites all over the world. Buildings and landmarks of great value are destroyed and removed each day. Therefore, documentation and recoding with the best methods available (CRP and TLS) is pertinent for the restoration and reconstruction of these damaged sites. The main objectives of this study aim to:

1. Assesses the accuracy of CRP and TLS techniques for documentation of two cultural heritage sites in Saudi Arabia, with reference to traditional surveying data and existing CAD drawings.
2. Construct digital 3D models of the two cultural heritage sites acquired by both techniques for site documentation.

1.4.Thesis Structure

The thesis is structured into 5 chapters: Chapter 1 is the Introduction where the problem statement and objectives of the research are presented. Chapter 2 provides the conceptual background of CRP and TLS techniques. In addition, this chapter covers the relevant research regarding the use of CRP and TLS in cultural heritage documentation. Chapter 3 presents the overall method for the two case studies in the Bab Makkah and Bab Sharif. Chapter 4 presents the experimental results to assess the accuracy of the CRP and TLS techniques for the two case studies. The thesis ends with conclusions of the research presented in Chapter 5.

CHAPTER 2: BACKGROUND

2.1.Introduction

This chapter reviews the principles of CRP, TLS, and traditional surveying techniques, as well as discusses previous uses of CRP and TLS. A comparison of TLS and CRP is presented with respect to some previous studies using CRP and TLS techniques for cultural heritage documentation.

2.2.Close Range Photogrammetry (CRP)

According to the Manual of Photogrammetry (Salam, 1980), CRP is a combination of art, science, and technology used to obtain precise mathematical measurements and three-dimensional (3D) data from two or more photographs. It is a measurement technique that calculates the 3D coordinates of an object from the measurements of two or more images of that object from different positions. The fundamental principle used in CRP is triangulation (Figure 2.1), which can be presented by collinearity equation as described in Equation 2.1.

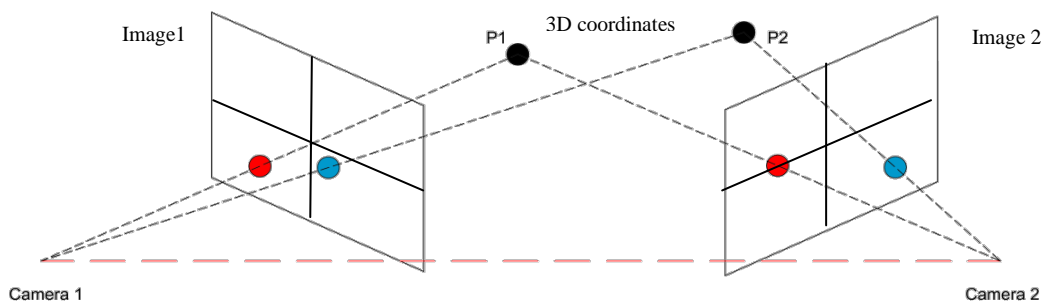


Figure 2.1. Photogrammetry principle

CRP follows two main steps:

1. Object (to be measured) data acquisition is performed by taking the required and necessary photos.
2. Processing the photos and producing maps or spatial coordinates.

If more than two photos are captured (Figure 2.2), a bundle adjustment solution is used, including all available measurements on the photos at the same time (Grussenmeyer and Hanke, 2002).

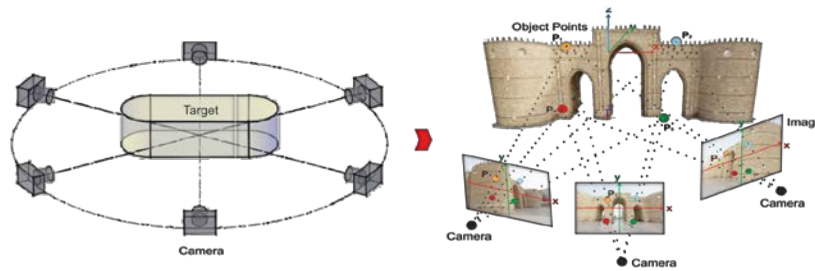


Figure 2.2. An example of configuration for a bundle solution

The collinearity equation (Equation 2.1) can be used in photogrammetry to relate coordinates from a two dimensional image to 3D object coordinate, as shown in Figure 2.3 (Salam, 1980).

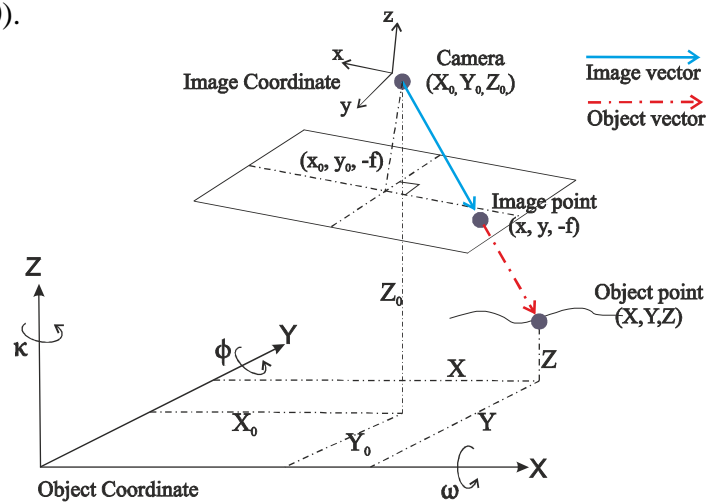


Figure 2.3. The Collinearity condition

$$\begin{aligned}
x &= x_0 - f \frac{r_{11}(X - X_0) + r_{21}(Y - Y_0) + r_{31}(Z - Z_0)}{r_{13}(X - X_0) + r_{23}(Y - Y_0) + r_{33}(Z - Z_0)} \\
y &= y_0 - f \frac{r_{12}(X - X_0) + r_{22}(Y - Y_0) + r_{32}(Z - Z_0)}{r_{13}(X - X_0) + r_{23}(Y - Y_0) + r_{33}(Z - Z_0)}
\end{aligned}
\tag{Eq. 2.1}$$

where:

- (X,Y,Z) are the object point coordinates
- (x, y) are the image coordinates
- The interior orientation parameters
 - (x_0, y_0) are the location of the principal point (offset)
 - (f) is the camera focal length
- The exterior orientation parameters
 - (X_0, Y_0, Z_0) are the projection center (camera location coordinates)
 - (r) is the rotation matrix with respect to the three orientation angles $(\omega, \varphi, \kappa)$

and

$$R = \begin{bmatrix} r_{11} & r_{21} & r_{31} \\ r_{12} & r_{22} & r_{32} \\ r_{13} & r_{23} & r_{33} \end{bmatrix}$$

$$= \begin{bmatrix} \cos \varphi \cos \kappa & -\cos \varphi \sin \kappa & \sin \varphi \\ \cos \omega \sin \kappa + \sin \omega \sin \varphi \cos \kappa & \cos \omega \cos \kappa + \sin \omega \sin \varphi \sin \kappa & -\sin \omega \cos \varphi \\ \sin \omega \sin \kappa - \cos \omega \sin \varphi \cos \kappa & \sin \omega \cos \kappa + \cos \omega \sin \varphi \sin \kappa & \cos \omega \cos \varphi \end{bmatrix}$$

- $[\Omega(\omega), \Phi(\varphi), \Kappa(\kappa)]$ are elements of image rotation around the three axes.

2.3. Terrestrial Laser Scanning (TLS)

Compared to CRP, TLS is a relatively new active remote sensing technique for 3D data acquisition. It is an active sensor technique referred to as Light Detection and Ranging (LiDAR) that can provide its own energy. It is now well-known for the precise measurements it provides and the accuracy it can achieve. TLS is one of laser scanning techniques that can be used for heritage building documentation. The basic measurement of any laser scanning system is based upon measuring the difference in time between the transmission and the reception of the laser pulse signal and the distance between the sensor and object.

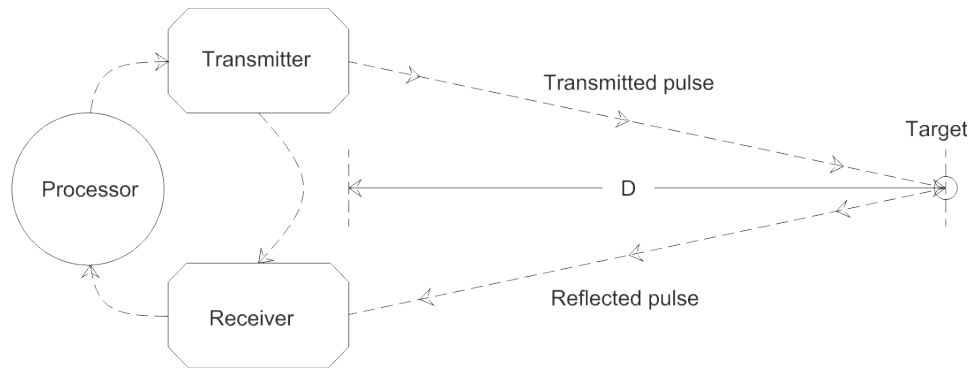


Figure 2.4. Concept of TLS measurements (Van Genechten, 2008)

The formula (Equation 2.2) used to measure the distance the pulse travels to the target and the time it takes to reflect it back (Figure 2.4) is described as follows:

$$D = \frac{(c \cdot t)}{2} \quad (\text{Eq. 2.2})$$

where:

D = distance

c = speed of light in the air

t = time between sending and receiving the signal

The laser scanner, in addition to the measurement of distance(ρ), also measures the horizontal and vertical angles, (α), as well as (θ) of the laser beam (Figure 2.5). The intensity of backscattered laser beam is also recorded. Equation 2.3 is used to convert those measurements into Cartesian coordinates.

$$\begin{bmatrix} x \\ y \\ z \end{bmatrix} = \rho \begin{bmatrix} \cos \theta \cdot \cos \alpha \\ \cos \theta \cdot \sin \alpha \\ \sin \theta \end{bmatrix} \quad (\text{Eq. 2.3})$$

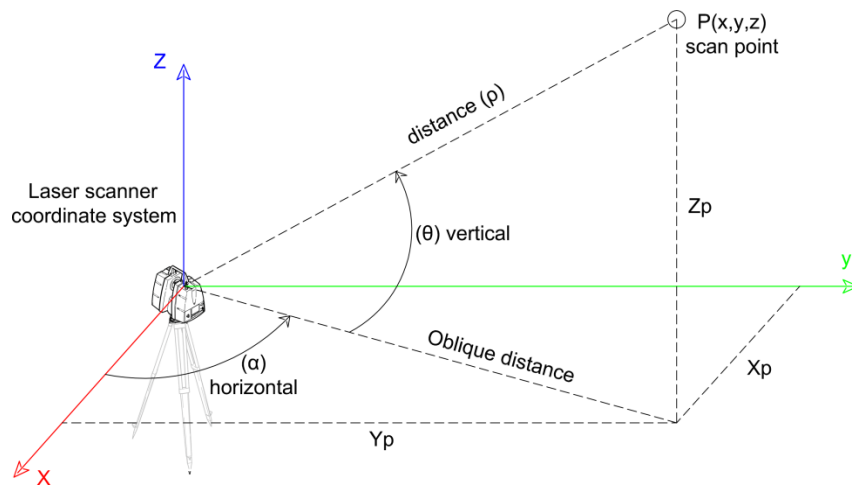


Figure 2.5. The principle of the Tacheometric laser

In any geodetic application, the most common transformation method used is the Helmert Transformation, also known as the Seven Transformations (Andrei, 2006). It performs coordinate transformations between two different Cartesian coordinate systems (Equation 2.4). For instance, the acquired coordinates for the surveyed objects are transformed from the TLS local coordinate system (X_1, Y_1, Z_1) to the real world projected coordinate system (X_2, Y_2, Z_2). The model considers the transformation parameters, including: three translations, three rotations, and a scale of the axes (Figure 2.6).

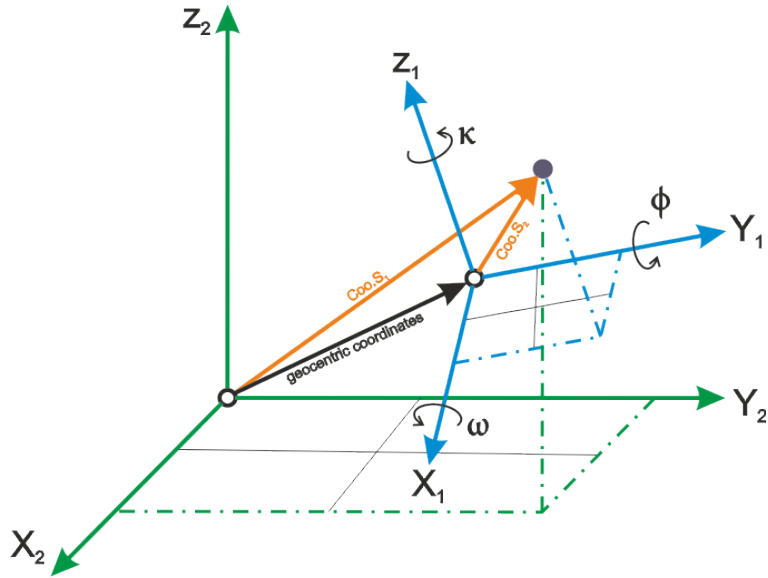


Figure 2.6. The seven transformation parameters

$$\begin{bmatrix} X_2 \\ Y_2 \\ Z_2 \end{bmatrix} = S R_{X_1}(\omega) R_{Y_1}(\phi) R_{Z_1}(\kappa) \begin{bmatrix} X_1 \\ Y_1 \\ Z_1 \end{bmatrix} + \begin{bmatrix} X_T \\ Y_T \\ Z_T \end{bmatrix} \quad (\text{Eq. 2.4})$$

where:

- $Coo.S_1, Coo.S_2$ refers to the point coordinates with respect to system 1 and 2.
- (X_2, Y_2, Z_2) are the geocentric coordinates with reference to the target datum (transformed coordinates vectors).
- (S) is the scale.
- $(R_{X_1}, R_{Y_1}, R_{Z_1})$ are the rotation matrices.
- (ω, ϕ, κ) are the rotation angles around $X_1, Y_1,$ and $Z_1,$ respectively.
- (X_1, Y_1, Z_1) are the 3D coordinates of system 1 (initial coordinates' vectors).
- (X_T, Y_T, Z_T) are the translations parameters.

2.4.Traditional Survey Using Leica Smart-Station (LSS)

Leica Smart-Station (LSS) is a smart tool that combines traditional total-Station (TPS 1200) and GPS devices (Leica Geosystems, 2005). During the surveying process with Leica Smart-Station, two controls points have to be used as a baseline in order to set up the Smart-Station orientation and coordinate system. The position at the first point (P1) should be determined with GPS. The surveyor should then orient to a second point (P2) that should be the backsight. Meanwhile, P1 will be the location that the smart station is set up. When the bearing between P1-P2 is known, all of the detail points surveyed will automatically be surveyed with respect to the predefined coordinate system. The process continues in the same way where the surveyor orients to P1 as backsight, in order to calculate the azimuth (Leica Geosystems, 2007); and then, surveys the rest of the targets from P2 (Figure 2.7). All points to be measured using Smart-Station can be measured from one or more base stations. More stations can be added depending on the site and the visibility to all points on the site.

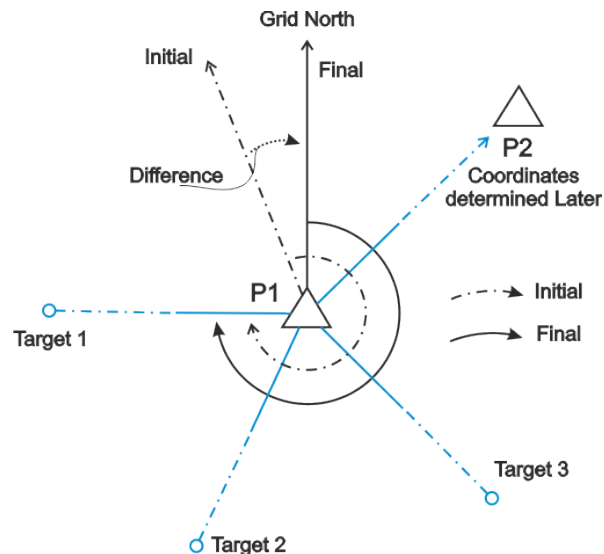


Figure 2.7. An illustration of a traditional survey using LSS (Leica Geosystems, 2007)

2.5. Close Range Photogrammetry (CRP) vs. Terrestrial Laser Scanning (TLS)

Photogrammetry and laser scanning are the two best-known remote sensing technologies for high resolution 3D data acquisition. The two techniques provide a number of advantages and disadvantages to the practitioners. High redundancy in photogrammetry is one of the main advantages, resulting in more accurate data. In addition, photogrammetry can be used to capture the façade of the target objects. Beside its redundancy and spatial information, the photogrammetry technique is considered cheaper and faster than TLS (Habib et al., 2004).

Conversely, TLS has an important advantage, the ability to provide direct extraction of 3D coordinates. Moreover, unlike photogrammetry, which has a passive sensor, laser scanning is equipped with an active sensor using its own energy, in turn, permitting data collection during the day and at night. Unfortunately, the high cost and amount of time needed to undertake laser scanning are two disadvantages, particularly when considering a smaller project (Habib et al., 2004). Table 2.1 summarizes the characteristics of photogrammetry and laser scanning.

Table 2.1. Characteristics of photogrammetry and laser scanner data

Characteristics	Photogrammetry	Laser Scanner
Modeling type	Image modeling	Range modeling
Cost of the instruments	Low	High
Time of data acquisition	Quite short	Long
3D information	To be derived	Direct
Scale	Absent	Present
Data volume	Images resolution	Dense point cloud
Texture	Included	Absent/Low resolution
Edges	Excellent	Quite problematic
Data collection	Day time only	Day or night
3D coordinates acquisition	Complicated	Direct

2.6.Existing Studies of Heritage Documentation

The main goal of heritage documentation is to record the geometry of a structure so that it can be used for maintenance, restoration, reconstruction, conservation, or educational purposes. Yilmaz et al. (2007) summarized four existing techniques for heritage documentation, including: the traditional manual method, topographic surveying, photogrammetry, and laser scanning. The traditional surveying method mainly utilizes hand-held measurement tools (e.g. tape) to perform on-site measurement of the dimensions of structures. Nevertheless, manual measurement is time-consuming and labor intensive. In addition, direct contact with the heritage structure during measurement may destroy the integrity of the structure unintentionally. Therefore, other alternatives have been introduced for heritage documentation in order to avoid such direct contact.

2.6.1. The Use of CRP for Heritage Documentation

CRP has been used for heritage documentation due to its accuracy and ability to record building texture information. A number of case studies have reported the documentation and restoration of heritage buildings such as: agro-industrial buildings (Arias et al., 2006), a historic castle (Brunetaud et al., 2012), and a fire-damaged historical building (Yilmaz et al., 2007). Yilmaz et al. (2008) used CRP measurements to document a historical building in Konya, Turkey, which had been destroyed by fire. A digital 3D model was constructed using the CRP data, which was used to restore the building after the accident.

Fuhi et al. (2009) used the CRP technique to document an archaeological site in Ajina Tepa, Tajikistan. The RMSE accuracy achieved was within 0.1 m throughout the entire

site. Hendrickx et al. (2011) researched the use of an unmanned aerial vehicle to mount a CRP system in order to survey the Tuekta burial mounds in the Russian Altay. The RMS error achieved was within 0.077-to-0.082 m. However, all the aforementioned studies did not perform or report any laboratory or on-site camera calibration, which is an important step to increase the accuracy of the photogrammetric product (Fraser 1997).

2.6.2. The Use of TLS for Heritage Documentation

The TLS technique has been used recently for the acquisition of information on heritage structures due to its ability for a massive collection of data point cloud. Such a technique can collect the geometric details of a structure on very fine scale, which can compensate for the drawbacks of CRP, especially when dealing with a complex structure and architecture (Haddad 2011). Al-kheder et al. (2009) combined the use of CRP and TLS to acquire the 3D structure of Amra, located in a desert area in Jordan. Lerma et al. (2010) performed a similar study using both techniques to document a natural environment – the upper Palaeolithic Cave of Parpalló - that is suited on top of a rugged terrain surface. Both techniques are used efficiently to produce a high quality 3D model with high geometric accuracy and visual quality.

Rüther et al. (2009) performed a large scale heritage conservation mapping of both the inside and outside of the Wonderwerk Cave in South Africa using TLS. The applied technique is able to relate the interior of the cave to its exterior, investigate the Cosmogenic burial dating, and pave the way for future conservation and development. In another application, Lubowiecka et al. (2009) combined the use of TLS and ground penetrating radar to model a historic bridge structure so as to estimate the structural

behavior for further maintenance. With the aid of finite element modelling, an assessment of the structural dynamics of the Cernadela Bridge can be achieved for rehabilitation and maintenance. Armesto-González et al. (2010) further demonstrated the use of the TLS intensity data to detect the potential damage within historical buildings. By applying a fuzzy k-means algorithm on the 2D intensity image, the suspicious location of cracks and damage can be located.

2.6.3. CRP vs. TLS for Heritage Documentation

Despite the extensive use of CRP and TLS techniques for heritage documentation, few attempts were reported of comparing the accuracy achieved by the two techniques. Nuttens et al. (2011) compared the CRP (using Canon EOS 1Ds) and TLS (Leica ScanStation 2) measurements for Sint-Baads Abbey, Flanders, Belgium. The RMSE achieved using CRP and TLS with respect to the use of total station measurements was 0.04 m and 0.023 m, respectively. Grussenmeyer et al. (2008) compared the use of TLS and CRP on recording the data for the Haut-Andlau Castle, Bas-Rhin province, France. The results reported showed that the RMS achieved by CRP and TLS was 0.005 m and 0.007 m, respectively. In addition to these attempts, Boehler and Marbs (2004) assessed five case studies to compare both measurement techniques. They concluded that CRP is a perfect solution if the object has distinct textures with predominated point-or line-based structures, so as to produce an accurate façade of the object. Nevertheless, TLS definitely outperforms CRP when dealing with complex and irregular objects, such as sculptures and reliefs.

With respect to the aforementioned studies, the majority agrees that a combination of CRP and TLS techniques yields the best results for heritage documentation, if sufficient time and resources are available. Nevertheless, with respect to the increased volume of data, a fully-automatic approach is still desired in the research community so as to provide an efficient and one-off solution for reality-based surveying and 3D modeling of heritage structures (Remondino, 2011).

CHAPTER 3: METHODOLOGY

3.1. Introduction

This chapter presents the method and experimental work for documenting two historical sites in Saudi Arabia, Bab Makkah and Bab Sharif. Data collection and processing for CRP and TLS were carried out in August 2013 for the two sites in order to compare the two techniques. General workflow on the process of how the work was run was followed. Later in this chapter, data collection and processing from CRP and TLS techniques, which were obtained from the field work, is presented. Finally, a traditional survey technique is used as a reference to assess the accuracy of the 3D model generated from both the CRP and TLS techniques.

3.2. Study Areas

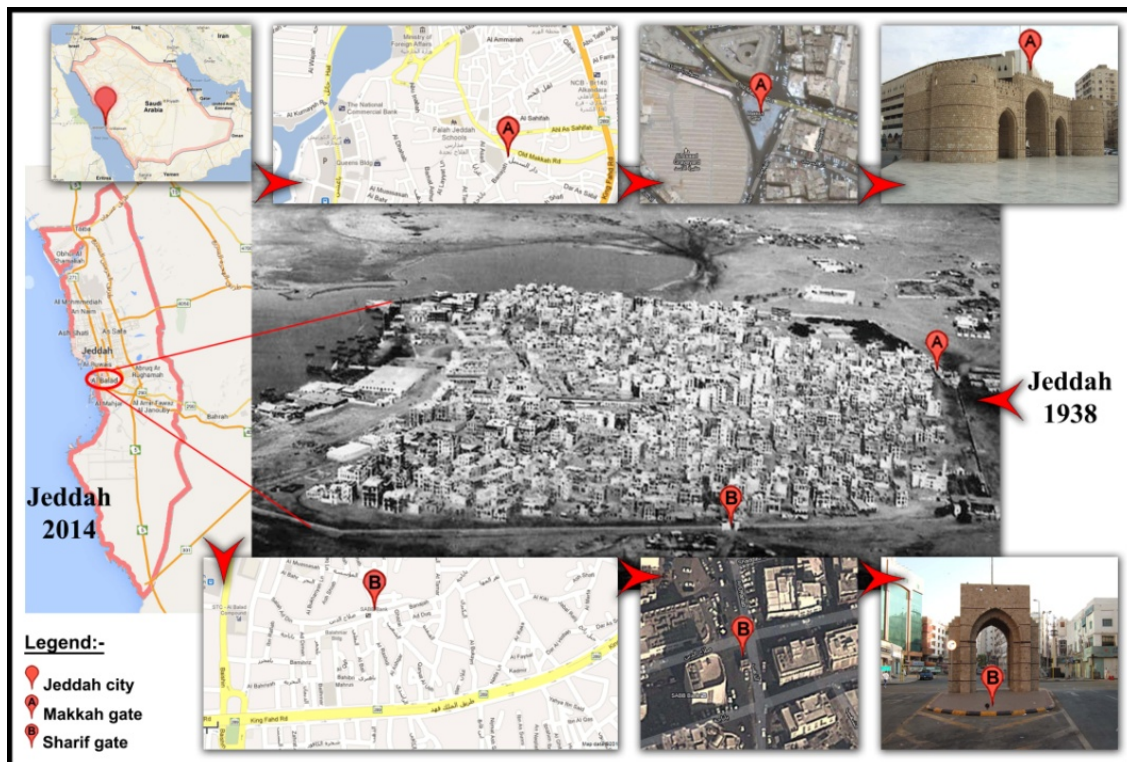


Figure 3.1. The historical region of Jeddah (Bab Makkah & Sharif Gate)

Jeddah has a remarkable mixture of modern and ancient history. About a century ago, Jeddah city was walled. This wall included six ancient gates which were originally implemented by Husain Al-Kurdi, one of the Mamluk princes, for the purpose of defense. The wall was totally removed in 1947, opening the way for the rapidly growing city, leaving the six gates to stand as historical landmarks. For the purposes of this study, I have chosen Bab Makkah and Bab Sharif, which in Arabic means “gateway to Makkah” and “gateway to Sharif”, respectively. These famous gates are located in historic district in downtown of Jeddah city. Both gates are mainly built using a stone, extracted from the sea, called 'Manqabi'. The gates were constructed by placing stones in rows, known as 'Madamik', and separating them by wooden intersection, called 'takail', in order to equally distribute the load on the walls.

Bab Makkah is considered a large gate. The gate size is 30m in length, 7m in width, and 8.50m in height. Unlike Bab Makkah, the size of Bab Sharif is relatively small, with a length of 4.39m, a width of 3.65m, and a height of 6.71m. Due to their historical significance both gates remain in their original position, which is now the middle of a street. Built in the 15th century, these two gates still attract a lot of attention; and thus, their appearance and maintenance are very important. Furthermore, these gates serve a purpose in the Islamic tradition, in that they have outstanding geometrical details (Figure 3.1).

3.3.General Workflow

Figure 3.2 and 3.3 show the general workflow for CRP, TLS, and traditional survey work:

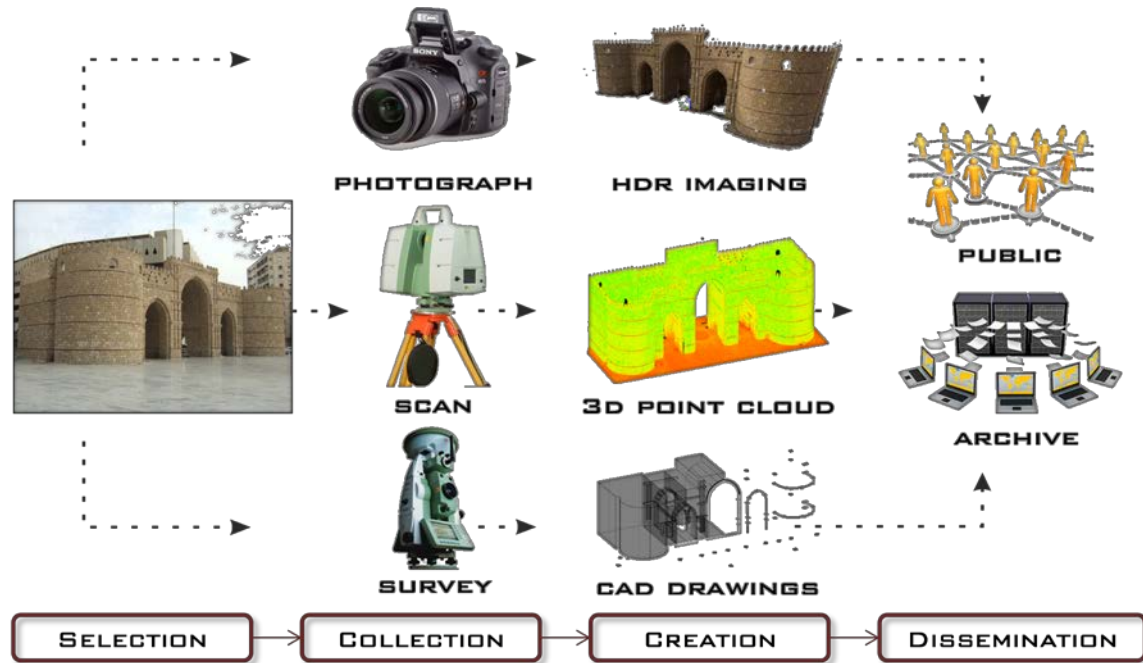


Figure 3.2. A pictogram illustration of general workflow

The four steps of the workflow:

1. Site selection was based on many factors such as construction size, architectural nature, building materials, and accessibility.
2. Field work has been done using the three methods including traditional survey, close-range photogrammetry, and 3D terrestrial laser scanning methods.
3. The collected data was used to create CAD drawings, High Dynamic Range photographs, 3D Point Clouds.
4. Each method was evaluated and compared across methods.

The procedure followed for each method is explained in the following section.

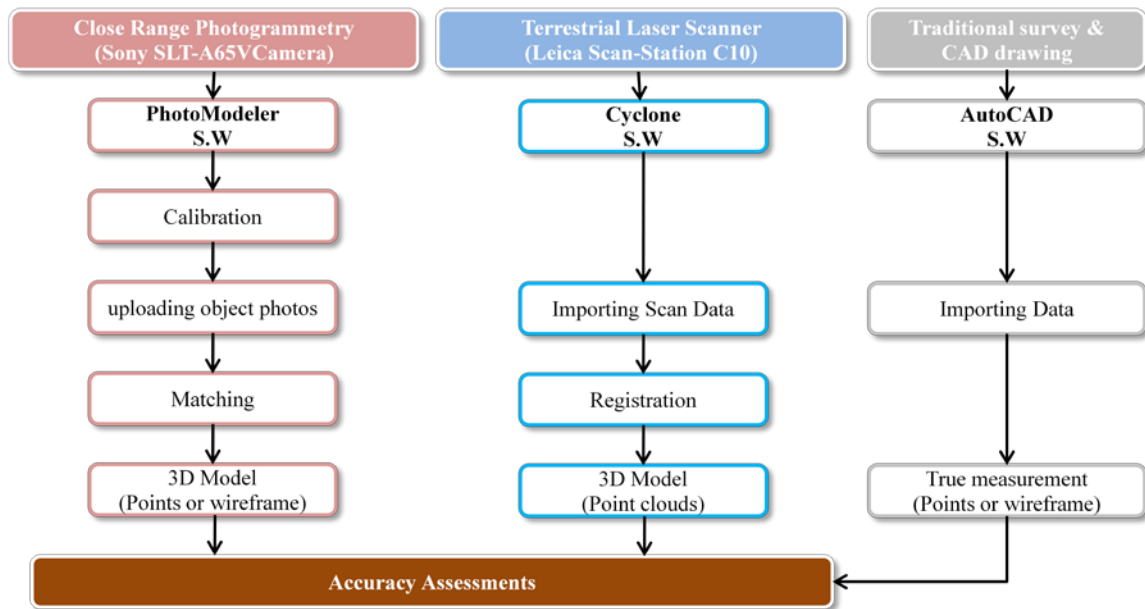


Figure 3.3. Research workflow

3.4. Close Range Photogrammetry (CRP)

Regarding the use of the CRP technique, a digital image processing software, called PhotoModeler, was used in both case studies. PhotoModeler is a software for close-range photogrammetry and image-based modeling. The software can be used to create 3D models from a set of images taken from the surveyed object (Jiang and Miao, 2011). Since PhotoModeler is an image-based modeling software, photography should be performed in a professional way where existing and artificial control points can easily be distinguished. Successive calibration and image processing in PhotoModeler are necessary for a successful outcome. Figure 3.4 shows the concept of digital close range photogrammetry.

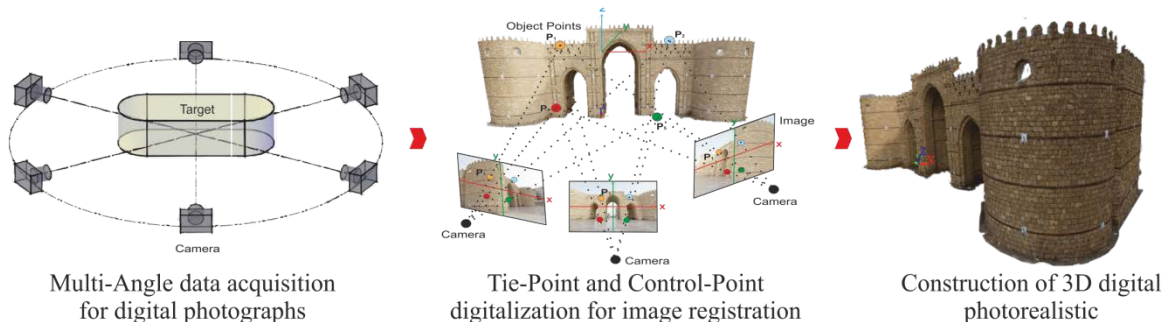


Figure 3.4. An illustration of close range photogrammetry concept

3.4.1. Data Acquisition for Bab Makkah and Bab Sharif

A Sony SLT-A65V camera was used to collect the imagery data for Bab Mekka. The camera was coupled with a 23.5 x 15.6 mm CMOS sensor, resulting in a 24.3 megapixel image. The CRP images were obtained by keeping the camera at the minimum focal length of 11 mm, while the highest level of the image resolution was set at 6000 x 4000 pixels. Since the study focuses on the large façade of the front of Bab Makkah, a total of 17 of images were taken and used for the CRP modeling. The distance between the camera and the gate was about 8-12 m from all stations. The images were taken in both landscape and portrait format for field calibration. The percentage of overlapping was about 93%.

Table 3.1. Camera specification

	Bab Makkah	Bab Sharif
Camera	Sony SLT-A65V	Fujifilm FinePix F10
Focal Length	11 mm	8 mm
Mesgapixels	24.3	6.3
Resolution	6000 x 4000	1549 x 2065

In order to test the influence of the use of professional camera verses unprofessional camera, a Fujifilm FinePix F10, was used to collect data about Bab Sharif. The camera

features 6.3 megapixels, with a 1/1.7" Super CCD HR sensor. Since the size of Bab Sharif is smaller than the Bab Makkah, a total of 7 images were sufficient to cover Bab Sharif. The images were obtained keeping the camera at the minimum focal length of 8 mm, while the highest level of the image resolution was set at 1549×2065 pixels in order to obtain high quality textures. The distance between the camera and the object was approximately 10 to 20 m from all stations. The percentage of overlap was about 83%.

3.4.2. Data Processing of Image Calibration

Camera calibration is an important step in any photogrammetric data collection. The purpose of camera calibration is to determine the exact values of camera parameters, such as focal length and lens distortion. In this study, two image calibration methods were carried out using PhotoModeller: Lab calibration and field calibration. The two calibration methods were used in order to test the effect of camera calibration on the overall accuracy.

3.4.2.1. Lab Camera Calibration

According to the instructions provided by PhotoModeller, a multi-sheet calibration should be used if the surveyed object is greater than a foot away (PhotoModeler Tutorial, 2013). Before taking the photos for calibration, all camera settings, such as resolution, zoom, and image quality, were retained as constant; while all other post-processing operations, such as sharpening and image stabilization were turned off. During image acquisition, the image scene was fully filled up with the photo window so that all parts of the camera lens were covered with at least one calibration sheet, as shown in Figure 3.5.

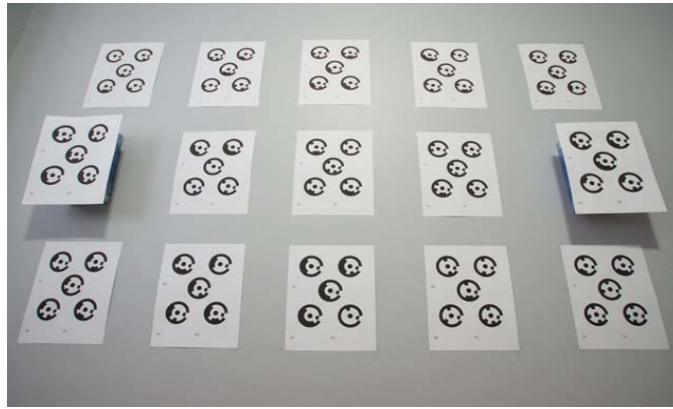


Figure 3.5. Multi-sheet lab camera calibration

Figure 3.6 shows an example of the automatic calibration process in PhotoModeler, as well as the 12 images taken by the digital camera (Sony SLT-A65V) for the calibration sheets. Firstly, four photos were taken at each side using a landscape orientation. After that, four more portrait photos were taken (the camera is rotated in a clockwise direction). In the last step, the camera was rotated in a counter-clockwise direction for the last four photos. All images were then added to a PhotoModler project, where auto-marking detected all the target points and solved for camera parameter, such as focal length and lens distortion.

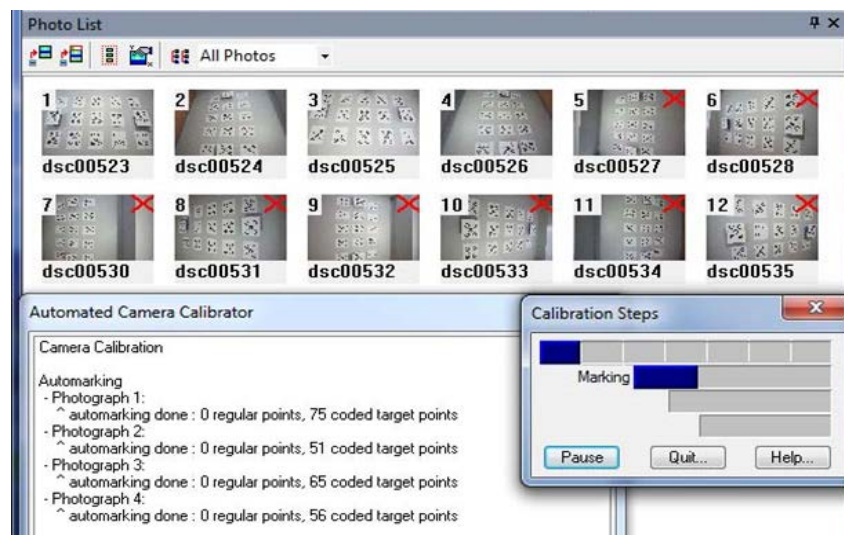


Figure 3.6. The automatic calibration process in PhotoModeler

Finally, the calibration report was generated. The overall RMS and maximum point marking residuals was 0.897 pixels and 3.432 pixels, respectively. According to the PhotoModeler tutorial guide (2013), a residual between 5 to 10 pixels can be considered high quality in a CRP project. Therefore, the residuals achieved were deemed within the acceptance level. The estimated focal length was 11.895 mm for the Sony camera.

Similar lab camera calibration was conducted for the Fujifilm FinePix F10 camera using a single-sheet calibration method. A total of 12 images were taken with similar settings to what has been mentioned previously. Finally, the RMS and maximum point marking residuals were calculated and found to be 0.126 pixels and 0.628 pixels, respectively, with an estimated focal length of 8.192 mm. Both calibration files were used as an input for post-processing of the CRP.

3.4.2.2. Field Camera Calibration

Field calibration is an alternative calibration method for fine tuning cameras in the field before the CRP is performed. When high accuracy is required, certain requirements have to be fulfilled in order to achieve accurate field calibration. For instance, 1) the camera parameters should be consistent during the shoot (no changes in zoom or focus); 2) the camera positions should cover a wide range of angles; 3) high redundancy of points should appear on photos from different angles; 4) all images should be consistently covered; 5) camera positions should be rolled in both landscape and portrait positions; and finally, 6) the targets or control points should also be clear and obvious.

According to the recommended settings of PhotoModeler, a field camera calibration was performed for the Bab Makkah to explore the effect of the camera field calibration

on result accuracy. Figure 3.7 shows the images taken for the field camera calibration for Bab Makkah. Though the camera was previously calibrated with a multi-sheet calibration approach (lab calibration) as mentioned in Section 3.4.2.1, the process was further improved by running the field calibration. Finally, the overall RMS of the point marking residual was 0.483 pixels, where the maximum residual was 0.994 pixels only.

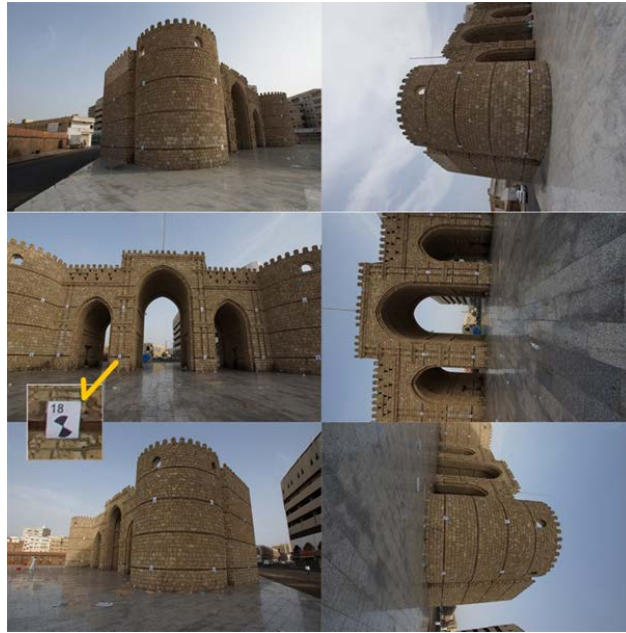


Figure 3.7. Example images used for field calibration

3.4.3. CRP Image Registration

After image calibration, CRP images are taken for the two sites, where image registration is performed in the PhotoModeller. By providing sufficient tie points and control points for the partially overlapping CRP images, the registration can be performed based on the use of the collinearity equation (Eq. 2.1), as mentioned in section 2.2. At least 3 control points (with known ground coordinates) should be provided for a pair of CRP images so as to solve the unknown transformation parameters in the collinearity equation, which thus register the CRP images into the ground coordinate system.

3.5. Terrestrial Laser Scanning (TLS)

TLS was conducted on Bab Makkah using Leica ScanStation C10. The device is configured with a wide field of view of 360° H \times 270° V, and pulse repetition rate up to 50,000 pts/s, with a 3D scan precision of 6 mm/50 m. The data processing software, Cyclone, was used to process the collected data point cloud and generate the 3D models.

3.5.1. Data Acquisition

There were a total of five scans conducted on Bab Makkah, using twenty 6" black & white targets, resulting in a dataset of 35,173,299 points. These scans (Figure. 3.8) captured an external perspective of the gate at a distance of 8 - 12 m. At least three visible targets were set up in each scan, so that geo-registration could be performed to combine all the scans. The collected data was stored in the scanner and transferred to a laptop for post-data processing using Cyclone.

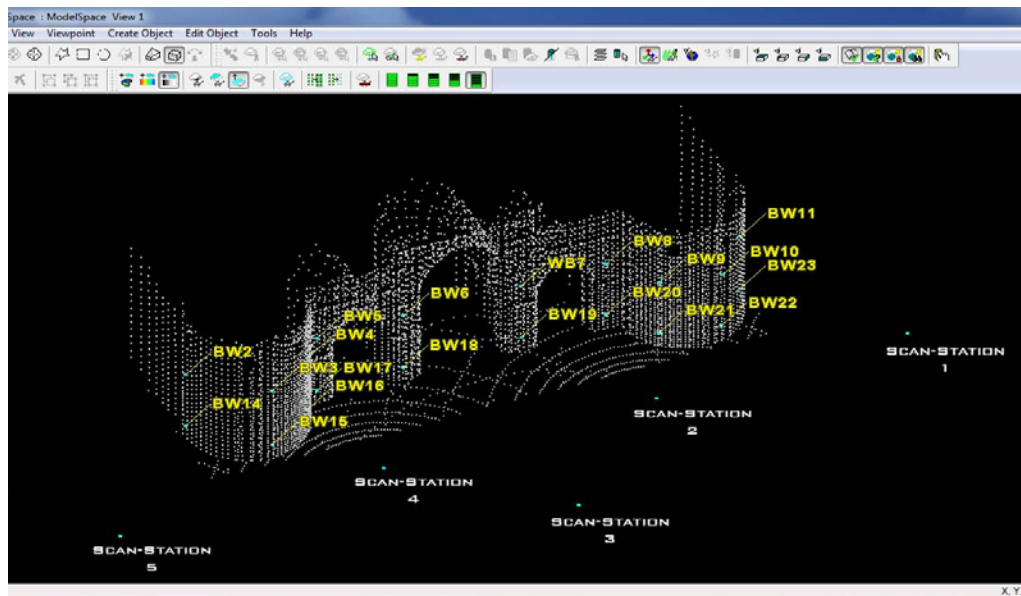


Figure 3.8. An illustration of the laser scanning configuration and the targets used

For Bab Sharif, five laser scans were carried out using four 6" circular tilt & turn targets. The data set comprises 25,208,377 points. The first four scans (as shown in Figure. 3.9) that captured the external surface of the gate were performed with a distance of 10 m to 20 m. An additional scan was setup inside the center of the gate so as to capture the structure under the gate. Similar to the above TLS work, at least three targets were used in each scan in order to register and combine all the five scans together.

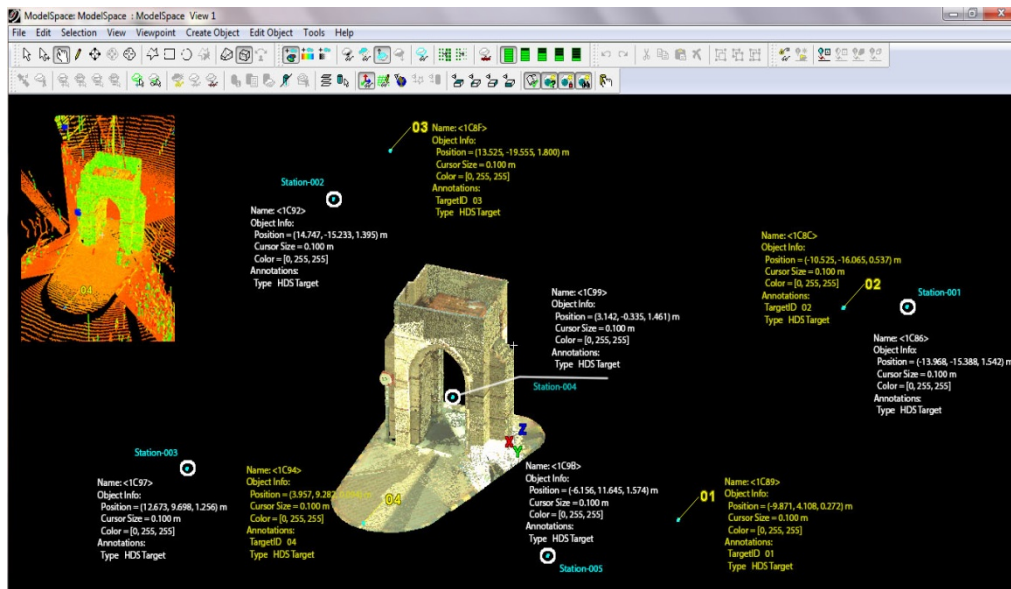


Figure 3.9. An illustration of the TLS in the Bab Sharif

3.5.2. Data Processing

The TLS data processing for Bab Makkah and Bab Sharif followed the same procedure. All five data scans were imported into the Cyclone software for data registration of the collected data point cloud. The data registration aims to use the common targets falling within the overlapping scans in order to align all the TLS data points into the ground coordinate system, based on the Equation. 2.4. By using the seven-parameter transformation, the acquired TLS data point cloud are geo-registered in the ground coordinate system by considering the translation, rotation and scale factors. As

shown in Figures 3.10 and 3.11 for tables captured from Cyclone S/W, the overall registration error ranges from 0.001 m to 0.002 m. The error represents the registration error between the targets aligned within the overlapping scans. According to the user guide of Cyclone, the registration error should be lower than 0.006 m so as to produce a high quality data point cloud model (Cyclone, 2008). Therefore, the results obtained in both case studies were deemed to be within the acceptable level of accuracy. After the registration, the data points falling outside the study structure are removed, so that the constructed 3D model represents only Bab Makkah and Bab Sharif.

Constraint...	ScanWorld	ScanWorld	Error
BW8	Station-003: SW-001 (Leveled)	Station-007: SW-001 (Leveled)	0.002 m
WB7	Station-003: SW-001 (Leveled)	Station-007: SW-001 (Leveled)	0.001 m
BW20	Station-003: SW-001 (Leveled)	Station-007: SW-001 (Leveled)	0.002 m
BW19	Station-003: SW-001 (Leveled)	Station-007: SW-001 (Leveled)	0.000 m
BW18	Station-002: SW-001 (Leveled)	Station-007: SW-001 (Leveled)	0.001 m
BW17	Station-002: SW-001 (Leveled)	Station-007: SW-001 (Leveled)	0.001 m
BW6	Station-002: SW-001 (Leveled)	Station-007: SW-001 (Leveled)	0.001 m
BW5	Station-002: SW-001 (Leveled)	Station-007: SW-001 (Leveled)	0.002 m
BW26	Station-003: SW-001 (Leveled)	Station-004: SW-001 (Leveled)	0.001 m
BW25	Station-003: SW-001 (Leveled)	Station-004: SW-001 (Leveled)	0.001 m
BW27	Station-001: SW-001 (Leveled)	Station-002: SW-001 (Leveled)	0.000 m
BW29	Station-001: SW-001 (Leveled)	Station-002: SW-001 (Leveled)	0.001 m
BW28	Station-001: SW-001 (Leveled)	Station-002: SW-001 (Leveled)	0.000 m
BW11	Station-004: SW-001 (Leveled)	Smart-Station 2,11,14,23 B.W. targets.txt (Leveled)	0.001 m
BW23	Station-004: SW-001 (Leveled)	Smart-Station 2,11,14,23 B.W. targets.txt (Leveled)	0.001 m
BW2	Station-001: SW-001 (Leveled)	Smart-Station 2,11,14,23 B.W. targets.txt (Leveled)	0.001 m
BW14	Station-001: SW-001 (Leveled)	Smart-Station 2,11,14,23 B.W. targets.txt (Leveled)	0.001 m

Figure 3.10. The results of data registration for Bab Makkah

The screenshot shows a software window titled "Registration: Register All Stations". The window has a menu bar with "Registration", "Edit", "ScanWorld", "Constraint", "Cloud Constraint", "Viewers", and "Help". Below the menu bar is a toolbar with various icons. The main area contains a tabbed interface with three tabs: "ScanWorlds' Constraints", "Constraint List", and "ModelSpaces". The "Constraint List" tab is active, displaying a table with the following data:

Cons...	ScanWorld	ScanWorld	Error
01	Station-001: SW-001 (Leveled)	Station-005: SW-001 (Leveled)	0.002 m
02	Station-001: SW-001 (Leveled)	Station-002: SW-001 (Leveled)	0.001 m
02	Station-001: SW-001 (Leveled)	Station-004: SW-001 (Leveled)	0.001 m
02	Station-001: SW-001 (Leveled)	Station-005: SW-001 (Leveled)	0.002 m
03	Station-001: SW-001 (Leveled)	Station-002: SW-001 (Leveled)	0.002 m
03	Station-001: SW-001 (Leveled)	Station-003: SW-001 (Leveled)	0.001 m
03	Station-001: SW-001 (Leveled)	Station-004: SW-001 (Leveled)	0.001 m
01	Station-001: SW-001 (Leveled)	Station-003: SW-001 (Leveled)	0.001 m
04	Station-002: SW-001 (Leveled)	Station-003: SW-001 (Leveled)	0.002 m
04	Station-002: SW-001 (Leveled)	Station-004: SW-001 (Leveled)	0.002 m
04	Station-002: SW-001 (Leveled)	Station-005: SW-001 (Leveled)	0.002 m
03	Station-002: SW-001 (Leveled)	Station-003: SW-001 (Leveled)	0.001 m
03	Station-002: SW-001 (Leveled)	Station-004: SW-001 (Leveled)	0.001 m
02	Station-002: SW-001 (Leveled)	Station-004: SW-001 (Leveled)	0.001 m
02	Station-002: SW-001 (Leveled)	Station-005: SW-001 (Leveled)	0.001 m
04	Station-003: SW-001 (Leveled)	Station-005: SW-001 (Leveled)	0.001 m
03	Station-003: SW-001 (Leveled)	Station-004: SW-001 (Leveled)	0.001 m
01	Station-003: SW-001 (Leveled)	Station-005: SW-001 (Leveled)	0.002 m
04	Station-003: SW-001 (Leveled)	Station-004: SW-001 (Leveled)	0.001 m
02	Station-004: SW-001 (Leveled)	Station-005: SW-001 (Leveled)	0.001 m
04	Station-004: SW-001 (Leveled)	Station-005: SW-001 (Leveled)	0.001 m

Figure 3.11. The results of data registration for Bab Sharif

3.6.Traditional Surveying

The Leica Smart-Station (LSS) was used to collect the target points installed on Bab Makkah in order to assess the accuracy of the same points collected by CRP and TLS. The measurements and the focus is given to those target points due to the unavailability of authorized 3D CAD drawings for Bab Makkah, which can be used as reference data to assess accuracy. Figure 3.12 illustrates the concept of data acquisition for Bab Makkah using the Smart-station. The LSS was set up in front of the gate in a location named station P1, where another backside station was setup as station P2. Since the Smart-station was equipped with GPS, the coordinates of these two points could be obtained in a global coordinate system (WGS84). In this case, a baseline was setup so that the 3D coordinates of the object points located on the gate could be surveyed with absolute coordinates. Finally, the 20 target points were collected for Bab Makkah in order to assess accuracy. It is worth mentioning that the 20 target points are evenly distributed within the structure and located at different parts of the structure. These points were then used to assess the accuracy of the object points measured by CRP and TLS.

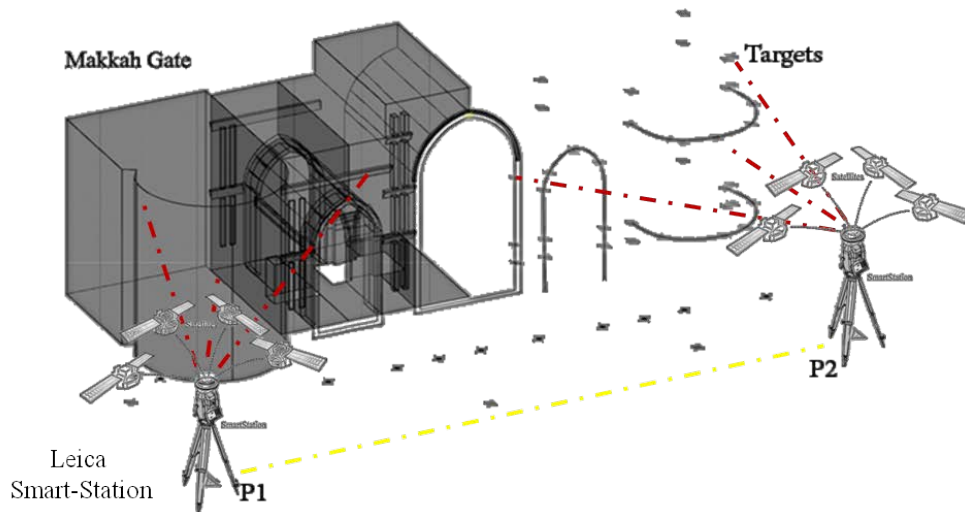


Figure 3.12. An illustration of traditional survey methods using Leica Smart Station

CHAPTER 4: RESULTS AND ANALYSIS

4.1.CRP Results of Bab Makkah Dataset

Seventeen images were collected and used for the 3D modeling of the gate using PhotoModeler Scanner software. The CRP images were matched using 164 natural control points located on different parts of the gate, such as wood edges and dots marking on the building materials. The points were matched and identified in order to create an accurate matching sequence for the images. The 20 artificial black and white targets, which were placed on the facade of the gate (Figures 4.1), were used for the accuracy assessment. However, in order to create a geo-registered 3D model, coordinates obtained from the Leica Smart-Station (Figures 4.2) for four artificial targets (points 2, 14, 11, and 23) were used during the image registration process.

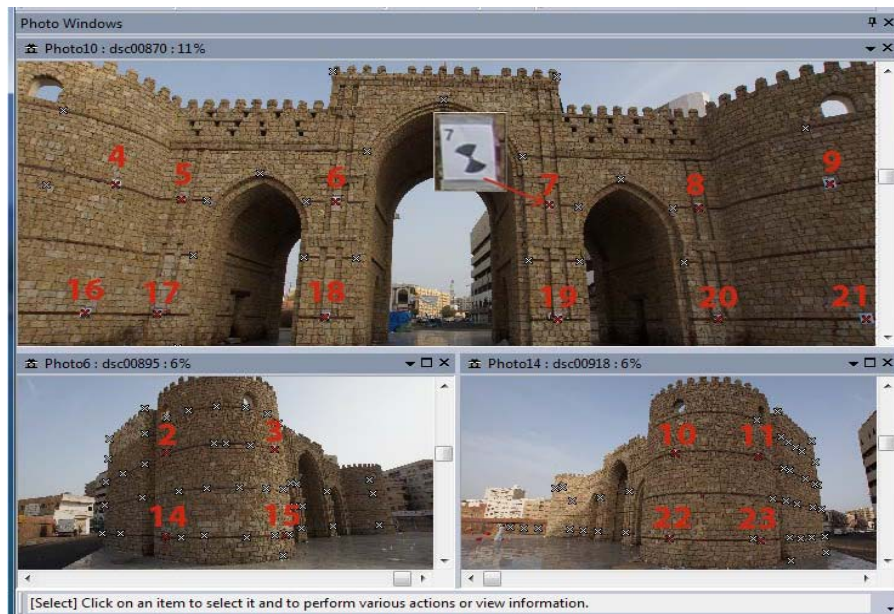


Figure 4.1. The distribution of 20 artificial black and white targets on Bab Makkah

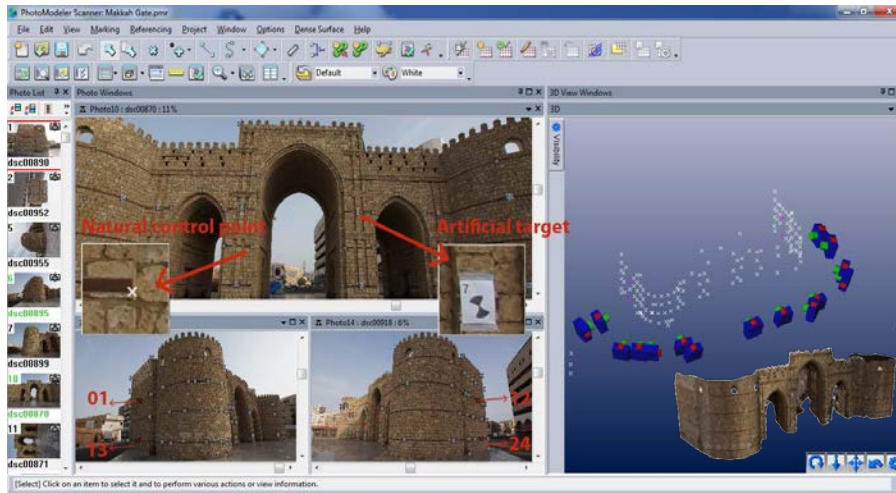


Figure 4.2. Four artificial targets that were assigned for image registration

4.2.CRP Results of Bab Sharif Dataset

Seven CRP images were used for the 3D modeling of the gate using PhotoModeler Scanner software. The first processing step involved matching 83 natural control points (wood edges) across different images. Unlike Bab Makkah, the detection of the reference features was done manually using PhotoModeler's point and line tools (Figure 4.3).

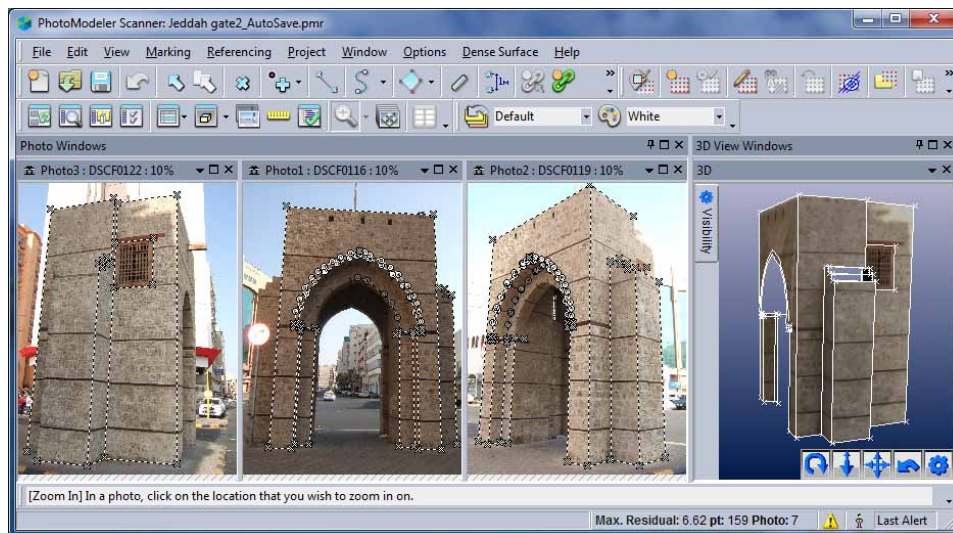


Figure 4.3. CRP image processing for Bab Sharif

The accuracy of the camera calibration results have been checked for both Bab Makkah and Bab Sharif. In Bab Makkah, lab and field calibration methods were used, while only lab calibration was used for Bab Sharif. Based upon lab calibration for Bab Makkah, the RMS calculated was 0.89 pixels, and the maximum residual was 3.43 pixels. To improve the camera performance, a field calibration was conducted. As a result, the projects maximum residual dropped to 0.994 pixels, and the overall RMS became 0.483 pixels. Meanwhile, the RMS and maximum point marking residuals for Bab Sharif using lab calibration only were 0.126 pixels and 0.628 pixels, respectively (See Table 4.1).

Table 4.1. Camera calibration results for Bab Makkah and Bab Sharif

	Lab calibration		Field calibration	
	Max. residuals (pixels)	RMS (pixels)	Max. residuals (pixels)	RMS (pixels)
Bab Makkah	3.430	0.890	0.994	0.483
Bab Sharif	0.628	0.126	Nil	Nil

4.3.TLS Results for Bab Makkah and Bab Sharif

In order to process the laser scanning data, the five scans of both Bab Makkah and Bab Sharif were imported and registered using Cyclone software (as mentioned in Section 3), which created a complete 3D model of point clouds as shown in Figures 4.4 and 4.5.

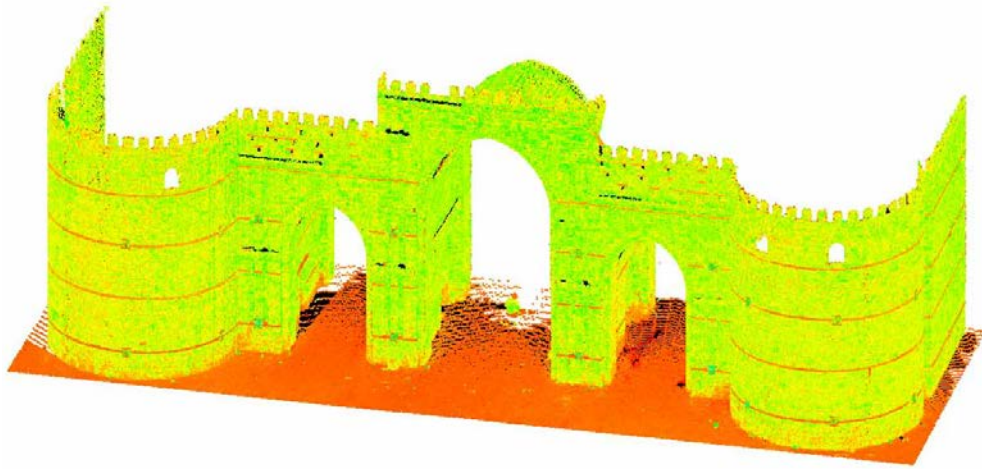


Figure 4.4. 3D model generation of Bab Makkah

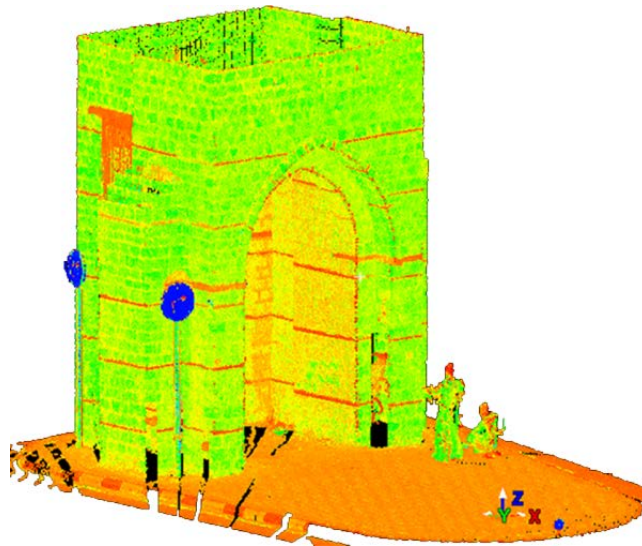


Figure 4.5. 3D model generation of Bab Sharif

4.4. Accuracy Assessment of Bab Makkah Results

Due to the lack of official government drawings or survey plans for Bab Makkah, the Leica Smart-Station was used to measure the artificial targets as reference data. The target measurements were used to evaluate the results obtained from the CRP and TLS methods. Table 4.2 shows the 3D coordinates measured for these 20 target points using the LSS and CRP, where the RMSE was computed between these two methods.

Table 4.2. Comparison between LSS and CRP coordinates of the same targets

Points	Traditional Survey (m)			Close Range Photogrammetry (m)						
	Leica Smart-Station			Sony a 65 Camera PhotoModeler Scanner S.W.			Residuals			RMS error
	X	Y	Z	X	Y	Z	dX	dY	dZ	
BW14	518926.531	2376894.205	5.866	518926.531	2376894.218	5.864	0.000	-0.013	0.002	0.013
BW02	518926.582	2376894.161	9.834	518926.583	2376894.160	9.835	-0.001	0.001	-0.001	0.002
BW03	518931.153	2376894.495	9.883	518931.166	2376894.488	9.892	-0.013	0.007	-0.009	0.017
BW15	518931.158	2376894.501	5.798	518931.170	2376894.503	5.796	-0.012	-0.002	0.002	0.013
BW05	518931.55	2376899.552	9.797	518931.5563	2376899.504	9.793	-0.006	0.048	0.004	0.048
BW17	518931.551	2376899.528	5.873	518931.5594	2376899.473	5.881	-0.008	0.055	-0.008	0.057
BW16	518931.716	2376897.929	5.856	518931.7175	2376897.89	5.861	-0.002	0.039	-0.005	0.039
BW04	518931.76	2376897.852	9.83	518931.7693	2376897.815	9.828	-0.009	0.037	0.002	0.038
BW18	518934.863	2376902.962	5.867	518934.8508	2376902.909	5.870	0.012	0.053	-0.003	0.055
BW06	518934.867	2376902.979	9.79	518934.8594	2376902.922	9.784	0.008	0.057	0.006	0.058
BW07	518939.393	2376907.608	9.738	518939.3743	2376907.549	9.733	0.019	0.059	0.005	0.062
BW19	518939.414	2376907.624	5.866	518939.3929	2376907.567	5.865	0.021	0.057	0.001	0.061
BW20	518942.67	2376910.973	5.848	518942.6508	2376910.91	5.845	0.019	0.063	0.003	0.066
BW08	518942.69	2376910.98	9.737	518942.6687	2376910.931	9.738	0.021	0.049	-0.001	0.053
BW21	518945.686	2376910.617	5.839	518945.6849	2376910.517	5.838	0.001	0.100	0.001	0.100
BW09	518945.748	2376910.609	9.716	518945.7693	2376910.508	9.701	-0.021	0.101	0.015	0.105
BW11	518948.062	2376915.845	9.663	518948.0614	2376915.844	9.672	0.001	0.001	-0.009	0.009
BW23	518948.113	2376915.739	5.826	518948.1133	2376915.727	5.816	0.000	0.012	0.010	0.015
BW22	518948.417	2376912.414	5.875	518948.4331	2376912.386	5.865	-0.016	0.028	0.010	0.034
BW10	518948.475	2376912.501	9.671	518948.4946	2376912.482	9.681	-0.020	0.019	-0.010	0.029
Total RMS error							0.011	0.040	0.005	0.044

As shown in Figure 4.1, ten of the target points are located in the lower portion of the structure (approximately 5 m above the measurement datum) and the other half of the 20 points are located in the upper portion (approximately 10 m above the measurement datum) of Bab Makkah. The RMS errors using the CRP technique of the control points are 0.011 m, 0.04 m and 0.005 m in X, Y, and Z directions, respectively. Results also show that the minimum errors of X, Y and Z are 0 m, 0.001 m, and 0.001 m, respectively; while the maximum error reaches 0.021 m, 0.1 m, and 0.015 m in the X, Y, Z directions (as shown in Table 4.2).

The minimum RMSE of all the points is 0.005 m where the maximum RMSE reaches up to 0.040 m, resulting in an overall RMSE of 0.044 m. One should note that the relatively large RMSE values are found at points BW09 and BW21 (Figure 4.6), on the right side of the main entrance of Bab Makkah. Due to the low contrast of photos taken at this portion, a relatively low number of matching points can be achieved in this curvy area. This situation thus degrades the geometric quality of the generated 3D model, resulting in a relatively high RMSE in Y direction close to 0.1 m.

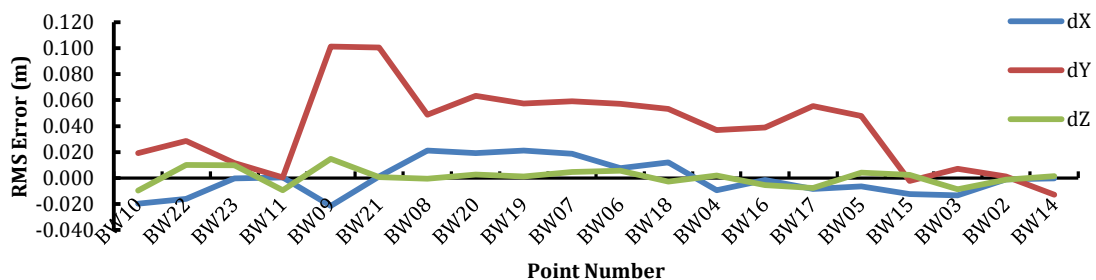


Figure 4.6. The RMS error produced by the CRP technique

Table 4.3. Comparison between LSS and TLS coordinates of the same targets

Points	Traditional Survey (m)			Terrestrial Laser Scanning (m)						
	Leica Smart-Station			Leica Laser Scanner C10 Cyclone S.W.			Residuals			RMS error
	X	Y	Z	X	Y	Z	dX	dY	dZ	
BW14	518926.531	2376894.205	5.866	518926.530	2376894.205	5.866	0.001	0.000	0.000	0.001
BW02	518926.582	2376894.161	9.834	518926.583	2376894.161	9.834	-0.001	0.000	0.000	0.001
BW03	518931.153	2376894.495	9.883	518931.156	2376894.489	9.882	-0.003	0.006	0.001	0.003
BW15	518931.158	2376894.501	5.798	518931.162	2376894.496	5.800	-0.004	0.005	-0.002	0.004
BW05	518931.55	2376899.552	9.797	518931.544	2376899.533	9.797	0.006	0.019	0.000	0.006
BW17	518931.551	2376899.528	5.873	518931.548	2376899.508	5.874	0.003	0.020	-0.001	0.003
BW16	518931.716	2376897.929	5.856	518931.731	2376897.933	5.855	-0.015	-0.004	0.001	0.015
BW04	518931.76	2376897.852	9.83	518931.773	2376897.855	9.830	-0.013	-0.003	0.000	0.013
BW18	518934.863	2376902.962	5.867	518934.851	2376902.949	5.868	0.012	0.013	-0.001	0.012
BW06	518934.867	2376902.979	9.79	518934.858	2376902.964	9.790	0.009	0.015	0.000	0.009
BW07	518939.393	2376907.608	9.738	518939.376	2376907.599	9.738	0.017	0.009	0.000	0.017
BW19	518939.414	2376907.624	5.866	518939.396	2376907.616	5.865	0.018	0.008	0.001	0.018
BW20	518942.67	2376910.973	5.848	518942.648	2376910.969	5.848	0.022	0.004	0.000	0.022
BW08	518942.69	2376910.98	9.737	518942.669	2376910.975	9.737	0.021	0.005	0.000	0.021
BW21	518945.686	2376910.617	5.839	518945.692	2376910.606	5.840	-0.006	0.011	-0.001	0.006
BW09	518945.748	2376910.609	9.716	518945.755	2376910.596	9.716	-0.007	0.013	0.000	0.007
BW11	518948.062	2376915.845	9.663	518948.062	2376915.845	9.663	0.000	0.000	0.000	0.000
BW23	518948.113	2376915.739	5.826	518948.113	2376915.739	5.826	0.000	0.000	0.000	0.000
BW22	518948.417	2376912.414	5.875	518948.419	2376912.414	5.875	-0.002	0.000	0.000	0.002
BW10	518948.475	2376912.501	9.671	518948.477	2376912.502	9.670	-0.002	-0.001	0.001	0.002
Total RMS error							0.008	0.007	0.001	0.008

Table 4.4. A summary of the accuracy assessment between CRP and TLS

	CRP (m)			TLS (m)		
	dX	dY	dZ	dX	dY	dZ
Min error	0.000	0.001	0.001	0.000	0.000	0.000
Max error	0.021	0.100	0.015	0.022	0.02	0.001
RMS error	0.011	0.040	0.005	0.008	0.007	0.001

Table 4.3 shows the same 20 points measured by the Leica Smart Station and TLS. The RMS errors of the target point residuals are 0.008 m, 0.007 m, and 0.001 m in X, Y, and Z directions, respectively. Results also show that the minimum error using the TLS for Bab Makkah in X, Y, and Z are all close to zero; while the maximum error reaches to 0.022 m, 0.02 m, and 0.002 m, in X, Y, Z directions, respectively. Overall, the RMSE calculated at the target points is better than those obtained measured by the CRP technique (Table 4.4). The overall RMSE is 0.008 m with a maximum RMSE of 0.008 m and minimum RMSE of 0.001 m. Comparing to the results obtained with CRP, there is no notable fluctuation of the RMSE among the 20 points (Figure 4.7).

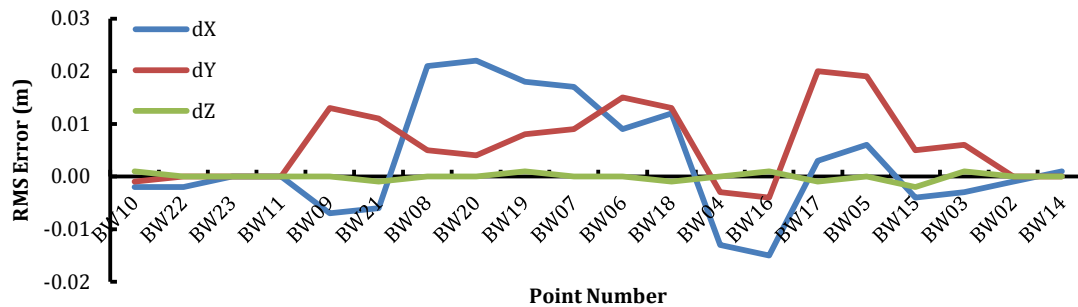


Figure 4.7. The RMS error produced by the TLS technique

The results summarized in Tables 4.2 and 4.3 represent the RMSE for each targeted point. The overall RMSE value for CRP is 0.044 m, where the overall RMSE value for TLS is 0.008 m.

The results achieved also demonstrate that the RMS error achieved using CRP is always higher than that obtained using TLS. The minimum difference between these two methods is found at point BW02. However, a significant difference in the RMS error is observed in points BW09 and BW21, where the difference is up to 0.1 m. One should note that BW09 and BW21 are located on the curvy structure of Bab Makkah (Figure 4.8). If the heritage structure has a large portion of irregular components, TLS should be used in order to achieve higher accuracy.

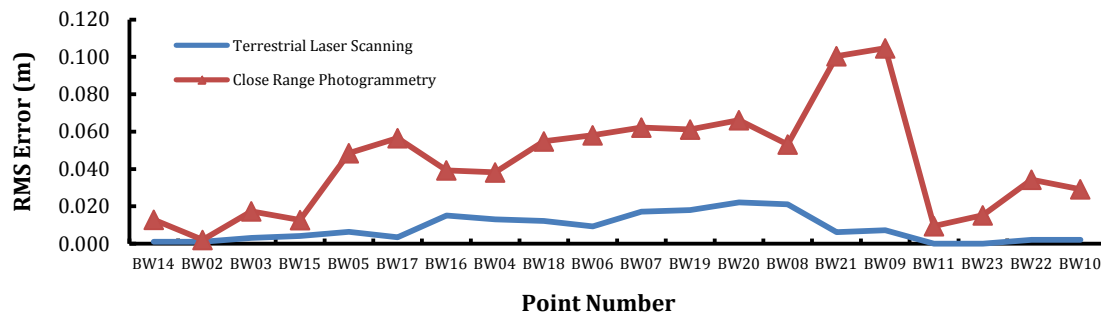


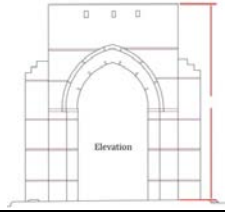
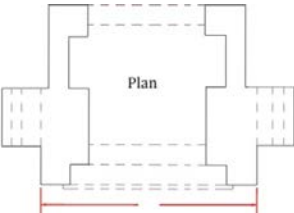
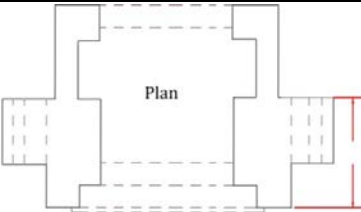
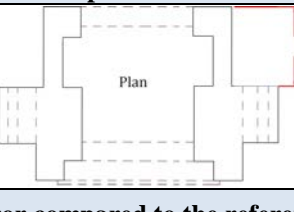
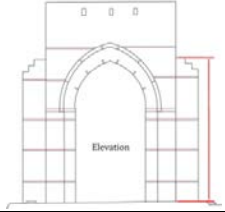
Figure 4.8. A comparison of RMS error between CRP and TLS

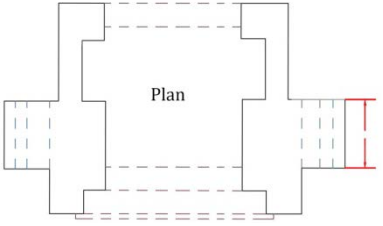
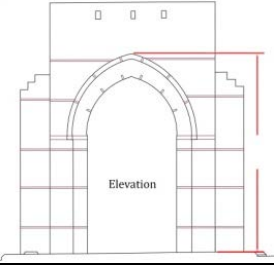
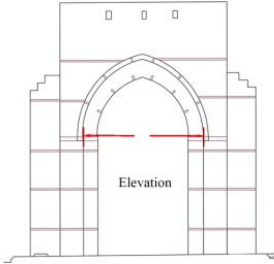
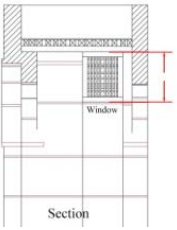
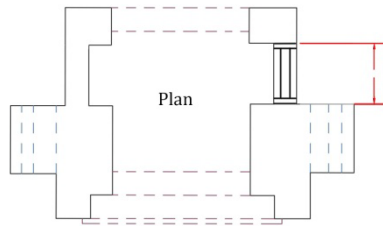
4.5. Accuracy Assessment of Bab Sharif Results

Table 4.5 shows ten selected measurements for dimensions on Bab Sharif. The accuracy of the CRP and TLS methods are evaluated by measuring different length on the gate based upon the unavailability of geo-referenced coordinates or point measurements. In addition, it was decided to use another evaluation tool by measuring distances on the gate considering that AutoCAD drawings were available for the gate. The measurements

performed on the gate included: the width of the window, height of the arch, and width of the gate. Table 4.6 summarizes the minimum, maximum, and average errors derived from the CRP and TLS methods in relation to the AutoCAD drawing provided by authorities.

Table 4.5. Accuracy assessment for Bab Sharif results

Output	Close Range Photogrammetry	Terrestrial Laser Scanner	(Reference)
	PhotoModeler Software	Cyclone Software	AutoCAD Software
	6.698 m	6.737 m	6.71 m
Error compared to the reference	0.012 m	- 0.027 m	
	4.395 m	4.396 m	4.39 m
Error compared to the reference	- 0.005 m	-0.006 m	
	1.988 m	1.992 m	1.98 m
Error compared to the reference	-0.008 m	- 0.012 m	
	1.661 m	1.662 m	1.67 m
Error compared to the reference	0.009 m	0.008 m	
	4.819 m	4.851 m	4.82 m
Error compared to the reference	0.001 m	-0.031 m	

Output	Close Range Photogrammetry	Terrestrial Laser Scanner	(Reference)
	PhotoModeler Software	Cyclone Software	AutoCAD Software
 <p>Plan</p>	1.178 m	1.177 m	1.19 m
Error compared to the reference	0.012 m	0.013 m	
 <p>Elevation</p>	5.364 m	5.374 m	5.34 m
Error compared to the reference	-0.024 m	- 0.034 m	
 <p>Elevation</p>	3.226 m	3.190 m	3.16 m
Error compared to the reference	-0.066 m	-0.03 m	
 <p>Window</p> <p>Section</p>	1.308 m	1.300 m	1.29 m
Error compared to the reference	-0.018 m	-0.01 m	
 <p>Plan</p>	1.053 m	1.032 m	1.03 m
Error compared to the reference	-0.023 m	-0.002 m	

Based on the results presented in Table 4.5, the RMS error using TLS is 0.021 m; whereas, the overall RMS error achieved by using the CRP is 0.025 m. Such a result is better than some of the previous studies, such as Nuttens et al. (2011), where the RMS error achieved was 0.04 m and 0.023 m using CRP and TLS, respectively. Table 4.6 summarizes the minimum, maximum, and overall RMS error of Bab Sherif's measurements. It is still noted that the TLS method produces better accuracy in comparison to CRP. However, the improvement of the accuracy achieved using TLS, in this case, is less than what had been achieved for Bab Makkah. This change in accuracy can be justified by the differences between the two data sets in terms of how the data is collected and the equipment used.

Table 4.6. A comparison of accuracy assessment achieved between CRP and TLS

	CRP (m)	TLS (m)
Min error	0.001	0.002
Max error	0.066	0.031
Average error	0.010	0.013
Overall RMS Error	0.025	0.021

CHAPTER 5: CONCLUSIONS

In this study, two remote sensing techniques are used for heritage site documentation in two study sites in Saudi Arabia: Bab Makkah and Bab Sharif. Due to the historic value, availability of equipment and the uniqueness of structure of the two sites, they were both surveyed using two remote sensing techniques: close-range photogrammetry (CRP) and terrestrial laser scanner (TLS). The results of the two methods were compared with reference data taken from two different data sources. Due to the unavailability of existing authorized CAD drawings for Bab Makkah, the reference measurement was conducted using Smart-Station equipment. For Bab Sharif, the measurements performed by both CRP and TLS were compared against existing CAD drawings provided by local authorities. Finally, the geometric accuracies achieved by the two methods (CRP and TLS) are compared with reference to the CAD drawings and the Smart-Station measurements in order to report and recommend the best method for heritage site documentation.

For CRP, camera calibration was conducted in both case studies. Laboratory calibration was carried out before performing the survey, where the RMS error achieved was 0.89 pixel and 0.126 pixel for Bab Makkah and Bab Sharif, respectively. A field calibration further improved the results to 0.483 pixels in the case study of Bab Makkah, which is within the acceptable accuracy recommended by the CRP software. In order to evaluate the geometric accuracy, 20 evenly distributed survey points were selected on Bab Makkah and 10 geometric dimensions were selected from the CAD drawings of Bab Sharif.

Finally, the results showed that the RMS error achieved by TLS and CRP for Bab Makkah are found to be 0.008 m and 0.044 m, respectively. However, both TLS and CRP achieved similar RMS errors for Bab Sharif, 0.021 m and 0.025 m, respectively. Generally, it was found that TLS gave better results when compared to CRP, despite the use of lab/field calibration in both case studies, which improved the accuracy of the photogrammetric product. Maximum RMS errors in TLS were usually found on those object points located on the complex structure of the study sites; whereas high RMS errors in CRP were observed when those object points were extracted in the low contrast portion of the images.

Based on the results of this study, heritage site documentation should be conducted using both techniques. CRP is able to provide fruitful textural information of the surveyed sites, which can be used to generate a photorealistic 3D model for site documentation. The high density of TLS point cloud data can offer an accurate detailed architectural description for the study sites, which is hence capable of providing a direct solution for digital 3D modeling and site recovery. Therefore, both techniques should be considered complementary; rather than, adversarial. Further research should look for an efficient and one-off solution for reality-based surveying and 3D modeling of heritage structures through using such a combination of measurement techniques.

References

- Abdelhafiz, A. (2009). *Integrating digital photogrammetry and terrestrial laser scanning*. Inst. For Geodesy and Photogrammetry, Technical University Braunschweig, Germany. ISBN 3-926146-18-4. Online on Deutsche Geodätische Kommission (DGK), München 2009, ISBN 978-3-7696-5043-3.
- Alan Walford. (April 2006). *One Part in 300,000 Precision and Accuracy Discussion*. Report, Eos Systems Inc.
- Al-Kheder, S., Al-Shawabkeh, Y., & Haala, N. (2009). Developing a documentation system for desert palaces in Jordan using 3D laser scanning and digital photogrammetry. *Journal of Archaeological Science*, 36(2), 537-546.
- Alshawabkeh, Y., & Haala, N. (2004). Integration of digital photogrammetry and laser scanning for heritage documentation. *The International Archives of the Photogrammetry, Remote Sensing and Spatial Information Sciences*, 35(B5).
- Altuntas, C., and Yildiz, F. (2012). Range and image sensor combination for three dimensional reconstruction of objects or scenes. *Sensor Review*, 32(3), 236 - 244.
- Andrei C.O., (2006). *3D affine coordinate transformations*. MSc in Geodesy, School of Architecture and the Built Environment. Royal Institute of Technology 'KTH', Stockholm, Sweden.
- Arias, P., Herraiez, J., Lorenzo, H., & Ordonez, C. (2005). Control of structural problems in cultural heritage monuments using close-range photogrammetry and computer methods. *Computers & Structures*, 83(21), 1754-1766.
- Arias, P., Ordóñez, C., Lorenzo, H., & Herraiez, J. (2006). Methods for documenting historical agro-industrial buildings: a comparative study and a simple photogrammetric method. *Journal of Cultural Heritage*, 7(4), 350-354.
- Armesto-González, J., Riveiro-Rodríguez, B., González-Aguilera, D., & Rivas-Brea, M. T. (2010). Terrestrial laser scanning intensity data applied to damage detection for historical buildings. *Journal of Archaeological Science*, 37(12), 3037-3047.
- Barsanti, S. G., Remondino, F., & Visintini, D. (2012). Photogrammetry and Laser Scanning for archaeological site 3D modeling—Some critical issues. In *Proc. of the 2nd Workshop on 'The New Technologies for Aquileia'*, V. Roberto, L. Fozzati.
- Bartos, K., Pukanská, K., Gajdosik, J. and Krajnák, M. (2011). The Issue of Documentation of Hardly Accessible Historical Monuments by Using of Photogrammetry and Laser Scanner Techniques. In: *XXIIIrd International CIPA Symposium*, Prague, Czech Republic. September 12–16, 2011.

- Boehler, W., & Marbs, A. (2004). 3D scanning and photogrammetry for heritage recording: a comparison. In: *Proceedings of the 12th International Conference on Geoinformatics*, pp. 291-298.
- Borkowski, A., & Józków, G. (2012). Accuracy Assessment of Building Models Created from Laser Scanning Data. *ISPRS-International Archives of the Photogrammetry, Remote Sensing and Spatial Information Sciences*, 1, 253-258.
- Cyclone (2008). Cyclone 5.8.1. Technical Specification. Available at: www.leica-geosystems.com (Accessed June 4, 2014).
- Ebrahim, M. A. B. (2000). Determination of the Islamic art accuracy by using digital close range photogrammetry. *International Archives of Photogrammetry and Remote Sensing*, 33(B5/1; PART 5), 195-202.
- El-Tokhey, M. E., Abdel-Gawad, A. K., Mogahed, Y. M., & El-Maghraby, A. M. (2013). Accuracy Assessment of Laser Scanner in Measuring and Monitoring Deformations of Structures. *World Applied Sciences Journal*, 26(2), 144-151.
- Fraser, C. S. (1997). Digital camera self-calibration. *ISPRS Journal of Photogrammetry and Remote Sensing*, 52(4), 149-159.
- Fujii, Y., Fodde, E., Watanabe, K., & Murakami, K. (2009). Digital photogrammetry for the documentation of structural damage in earthen archaeological sites: The case of Ajina Tepa, Tajikistan. *Engineering Geology*, 105(1), 124-133.
- Geosystems, L. (2008). Cyclone 5.8. 1: *Comprehensive software for working with laser scan data*. San Ramon, Calif.
- Grussenmeyer, P., Landes, T., Voegtle, T., & Ringle, K. (2008). Comparison methods of terrestrial laser scanning, photogrammetry and tacheometry data for recording of cultural heritage buildings. In *ISPRS Congress Proceedings, Beijing*, 213-18.
- Grussenmeyer, P. & Hanke, K. (2002). *Architectural photogrammetry: Basic theory, Procedures, Tools*. ISPRS Commission 5 Tutorial.
- Habib, A. F., Ghanma, M. S., & Tait, M. (2004). Integration of LIDAR and photogrammetry for close range applications. In *Proceedings of the ISPRS XXth Conference, Istanbul, Turkey B* (Vol. 35).
- Haddad, N. & Akasheh, T. (2005). Documentation of archaeological sites and monuments: ancient theatres in Jerash. In *Proceedings of CIPA XXth International Symposium*, September 26–October 1, Torino, Italy, 350–355.
- Haddad, N. A. (2011). From ground surveying to 3D laser scanner: A review of techniques used for spatial documentation of historic sites. *Journal of King Saud University-Engineering Sciences*, 23(2), 109-118.

- Hendrickx, M., Gheyle, W., Bonne, J., Bourgeois, J., De Wulf, A., & Goossens, R. (2011). The use of stereoscopic images taken from a microdrone for the documentation of heritage—an example from the Tuekta burial mounds in the Russian Altay. *Journal of Archaeological Science*, 38(11), 2968-2978.
- Jiang, T., & Miao, X. (2011). Research and application of three-dimensional modeling based on Photomodeler Scanner. *Communications in Information Science and Management Engineering*.
- Kadobayashi, R., Kochi, N., Otani, H., & Furukawa, R. (2004). Comparison and evaluation of laser scanning and photogrammetry and their combined use for digital recording of cultural heritage. *International Archives of the Photogrammetry, Remote Sensing and Spatial Information Sciences*, 35(5), 401-406.
- Lee, S.Y., Majd, Z., and Setan, H. 2013. 3D data acquisition for indoor assets using terrestrial laser scanning. *ISPRS Annals of the Photogrammetry, Remote Sensing and Spatial Information Sciences*, Volume II-2/W1, pp. 221-226.
- Leica Geosystems (2005). Leica Smartstation - the Integration of GPS and Total Station Technologies. Available at <http://www.leica-geosystems.com/> (Accessed June 4, 2014)
- Leica Geosystems (2007). Combining TPS and GPS SmartStation and SmartPole - high Performance GNSS Systems. Available at <http://www.leica-geosystems.com/> (Accessed June 4, 2014)
- Lichti, D. (2007). Error modelling, calibration and analysis of an AM-CW terrestrial laser scanner system. *ISPRS Journal of Photogrammetry and Remote Sensing*, 61(5), 307–324.
- Lichti, D. D., & Licht, M. G. (2006). Experiences with terrestrial laser scanner modelling and accuracy assessment. *International Archives of Photogrammetry Remote Sensing and Spatial Information Sciences*, 36(5), 155-160.
- Luhmann, T., Robson, S., Kyle, S., and Harley, I. (2007). *Close Range Photogrammetry: Principles, Techniques and Applications*. Whittles Publishing. Caithness, Scotland, UK.
- Nuttens, T., De Maeyer, P., De Wulf, A., Goossens, R., & Stal, C. (2011). Terrestrial laser scanning and digital photogrammetry for cultural heritage: an accuracy assessment. In *FIG Working Week 2011: Bridging the gap between cultures*. International Federation of Surveyors (FIG).
- Pérez, M., Agüera, F., & Carvajal, F. (2011). Digital camera calibration using images taken from an unmanned aerial vehicle. *The International Archives of the Photogrammetry, Remote Sensing and Spatial Information Sciences*, 38(1), C22.

- PohotoModeler Tutorial (2013). PhotoModeler, Version 2013. Vancouver: Eos Systems Inc., 2013.
- Remondino, F. (2011). Heritage recording and 3D modeling with photogrammetry and 3D scanning. *Remote Sensing*, 3(6), 1104-1138.
- Renyi. L., Guigang. S., and Fengquan. J. (2010). *Ancient architecture reconstructing based on Terrestrial 3D Laser Scanning technology*. In: *Proceedings of the 2010 2nd International Conference on Software Engineering and Data Mining (SEDM)*, pp.285- 288.
- Rüther, H., Chazan, M., Schroeder, R., Neeser, R., Held, C., Walker, S. J., Matmon, A., & Horwitz, L. K. (2009). Laser scanning for conservation and research of African cultural heritage sites: the case study of Wonderwerk Cave, South Africa. *Journal of Archaeological Science*, 36(9), 1847-1856.
- Singh, S. P., Jain, K., & Mandla, V. R. (2013). Virtual 3D Campus Modeling by Using Close Range Photogrammetry. *American Journal of Civil Engineering and Architecture*, 1(6), 200-205.
- Slama, C. C., Theurer, C., & Henriksen, S. W. (1980). *Manual of photogrammetry* (No. Ed. 4). American Society of Photogrammetry and Remote Sensing.
- Tonon, F., & Kottenstette, J. T. (2006). Laser and photogrammetric methods for rock face characterization. In: *Report on a workshop held in Golden, Colorado*.
- Van Genechten, B. (2008). *Theory and practice on Terrestrial Laser Scanning: Training material based on practical applications*. Universidad Politecnica de Valencia Editorial.
- Yilmaz, H. M., Yakar, M., & Yildiz, F. (2008). Documentation of historical caravansaries by digital close range photogrammetry. *Automation in Construction*, 17(4), 489-498.
- Yilmaz. H.M., Yakar. M., and Gulec. S.A., and Dulgerler. O.N. (2007). Importance of digital close-range photogrammetry in documentation of cultural heritage. *Journal of Cultural Heritage*. 8 (4), 428-433.
- Zhan Z.Q. (2008). Camera calibration based on Liquid Crystal Display (LCD). *The International Archives of the Photogrammetry, Remote Sensing and Spatial Information Sciences*, 37.
- Zulkepli M., Setan, H., and Chong, A. K. (2009). Accuracy assessments of point cloud 3D registration method for high accuracy craniofacial mapping. *Geoinformation Science Journal*, 9 (2). pp. 36-44.